DOI:
10.1182/blood-2016-03-703702

Document Version
Peer reviewed version

Deep-phenotyping of Tregs identifies an immune signature for idiopathic aplastic anemia and predicts response to treatment.

Running title: Treg deep-phenotyping in AA for treatment response

Authors: Shahram Kordasti,[†1,2] Benedetta Costantini,[†1,2] Thomas Seidl,[†1] Pilar Perez Abellan,[2] Marc Martinez Llordella,[3] Donal McLornan,[2] Kirsten E. Diggins,[6] Austin Kulasekararaj,[2] Cinzia Benfatto,[1] Xingmin Feng,[4] Alexander Smith,[1,2] Syed A. Mian,[1] Rossella Melchiotti,[5] Emanuele de Rinadis,[5] Richard Ellis,[5] Nedyalko Petrov,[5] Giovanni A.M. Povoleri,[3] Sun Sook Chung,[1] N. Shaun B. Thomas,[1] Farzin Farzaneh,[1] Jonathan M. Irish,[6] Susanne Heck,[5] Neal S. Young,[4] Judith C W Marsh,[1,2] Ghulam J. Mufti[1,2]

Affiliations:

[1]Department of Haematological Medicine, King's College London, London, United Kingdom.

[2]Haematological Medicine, King's College Hospital, London, United Kingdom.

[3]Division of Transplantation Immunology & Mucosal Biology, King's College London, London, United Kingdom.

[4]Hematology Branch, National Heart, Lung, and Blood Institute, National Institutes of Health, Bethesda, MD, USA.

[5]NIHR Biomedical Research Centre, King's College London, London, United Kingdom.

[6]Department of Cancer Biology, Vanderbilt University, Nashville, TN 37232, USA

† Joint first authors

Text word count: 4090
Abstract word count: 205 words
Number of figures: 7 (11 supplementary)
Number of tables: 3 (3 supplementary)
Number of references: 52

Corresponding author: Professor Ghulam J. Mufti, Department of Haematological Medicine, King's College London, Rayne Institute, 123 Coldharbour Lane, London, United Kingdom, SE5 9NU; Phone: 44(0)2073463080; Fax: 44(0)2073463514; e-mail: ghulam.mufti@kcl.ac.uk.

Key points

- Mass cytometry reveals a Treg immune signature for aplastic anemia (AA), and for response to ATG**.**
- AA Tregs in vitro are expandable, stable and functional, with potential for future therapeutic options.

Abstract

Idiopathic aplastic anemia (AA) is an immune-mediated and serious form of bone marrow failure. Akin to other autoimmune diseases, we have previously shown that in AA regulatory T-cells (Tregs) are reduced in number and function. The aim of this study was to further characterize Treg subpopulations in AA and investigate the potential correlation between specific Treg subsets and response to immunosuppressive therapy (IST) as well as their *in-vitro* expandability for potential clinical use. Using mass cytometry (CyTOF) and an unbiased multidimensional analytical approach, we identified two specific human Treg subpopulations (Treg A and Treg B) with distinct phenotypes, gene-expression, expandability and function. Treg subpopulation B, predominates in IST responder patients, has a memory/activated phenotype (with higher expression of CD95, CCR4 and CD45RO within $FOXP3^{hi}$, $CD127^{lo}$ Tregs), expresses the IL-2/STAT5 pathway and cell-cycle commitment genes. Furthermore, *in-vitro* expanded Tregs become functional and with the characteristics of Treg subpopulation B. Collectively, this study identifies human Treg subpopulations that can be used as predictive biomarkers for response to IST in AA and potentially other autoimmune diseases. We also show that Tregs from AA patients are IL-2 sensitive and expandable *in-vitro*, suggesting novel therapeutic approaches such as low dose IL-2 therapy and/or expanded autologous Tregs and meriting further exploration.

Introduction

Treatment options for idiopathic aplastic anemia(AA) include allogeneic hematopoietic stem cell transplantation (HSCT) or immunosuppressive therapy (IST), and recently eltrombopag for refractory severe AA.[1-3] Some patients are ineligible for HSCT due to older age or lack of a suitable donor, and following IST a third of patients fail to respond and 35% relapse after responding. Up to 20% of patients transform to myelodysplastic syndrome (MDS) or acute myeloid leukemia (AML) after IST[3-7]. Additional novel therapeutic approaches are needed for AA patients who fail to respond to IST, and alongside this, more robust diagnostic tests that predict response to IST.

We, and others, have shown a reduction in the number and function of Tregs in AA[8-11]. Tregs from AA patients also secrete pro-inflammatory cytokines[8]. Correlation between number and function of Tregs and response to standard IST has not been fully investigated, and it is unclear whether the dominant Treg subpopulation in AA is more of a T conventional(T_{con}) subtype or are genuinely functional Tregs.

The aims of this study were (i) to identify an immune signature for AA compared to healthy individuals, based on Treg subpopulations and T_{con} (ii) to identify the immune signature that predicts response to IST at time of diagnosis of AA and (iii) to examine the expandability and characteristics of Treg subpopulations that may form the basis for novel therapeutic approach to AA patients who are refractory to IST. For this, we utilized a novel deep-phenotyping strategy using multi-parameter mass cytometry (known as cytometry by time-of-flight (CyTOF)) and automated clustering method including t-distributed stochastic neighbour embedding (t-SNE)[12] to visually (viSNE) identify cell populations[13] in combination with spanning-tree progression analysis of density-normalized events (SPADE)[14]. This enabled us to identify two distinct subpopulations of human Tregs in AA and healthy age matched donors (HDs), and to demonstrate clear differences in AA that predicted response to IST. We also showed that AA Tregs can be expanded *in-vitro* and that they are stable and functional.

Methods

Patients and healthy donors

Thirty-nine AA patients at diagnosis and 31 HDs were recruited(summarized in table-1). Peripheral blood mononuclear cells(PBMCs) from 16 patients (12 IST-responder and 4 non-responders) were used for initial CyTOF analysis and samples from another 15 patients(11 IST-responders and 4 non-responders) were used as validation cohort. PBMCs from additional 8 patients were used for functional assays in addition to 4 patients from the initial cohort. Response to IST was evaluated at 6 months post-therapy. Median age was 45 years (range 20-72 years). IST

eligible AA patients were randomly invited to participate in this study. All patients< 35 years old were screened for Fanconi anemia.

Antibodies and cell staining

We designed a panel of antibodies based on surface markers, transcription factors and cytokines (table-s1). Each antibody was tagged with a rare metal isotope and its function verified by conventional flow-cytometry prior to mass-cytometry (supplementary methods). CyTOF-2 mass cytometer(Fluidigm) was used for data acquisition. Acquired data were normalized based on normalization beads (Ce 140, Eu151, Eu153, Ho165 and Lu175).[15] Automated clustering was performed on a subset of 800,000 cells sampled from all individuals. The number of cells sampled from each individual was proportional to the total number of cells in that sample. Collected cells were stained with metal conjugated antibodies with or without a 4-hour stimulation with phorbol myristate acetate (PMA) and ionomycin in the presence of brefeldin. Intracellular staining for transcription factors and cytokines was performed after fixation and permeabilization according to manufacturer's instructions (eBioscience). Conventional flow-cytometry data were analyzed by polychromatic flowcytometer (LSRFortessa, BD biosciences).

Data processing, scale transformation, automated clustering and distance computations

Data were initially processed and analyzed using Cytobank.[16] The stand-alone analysis tool cyt was also used for performing t-SNE dimensionality reduction and merging distinct FCS files[13]. We analyzed mass-cytometry complex data using viSNE[12] to visually identify delineate subpopulations[13] in combination with SPADE[14] and heatmaps[15]. To distinguish $CD4^+$ T-cell subpopulations, in particular Tregs.[15] See the supplementary material and methods.

Treg expansion

Freshly isolated live Tregs were stimulated with anti CD3/CD28 beads(1:1 ratio) (Dynabeads human T-activator CD3/CD28, Life Technologies) and high dose(1,000 IU/ml) interleukin-2 (IL-2)(Proleukin, Novartis) for four weeks with all-trans retinoic acid(ATRA) 2 µM (Sigma Aldrich) and rapamycin(Rapa) 100 nM(Alfa-Aesar). Culture medium (XV Prime, Irvine Scientific supplemented with AB serum 10%) and beads was replenished every week. After 4 weeks of expansion, cells were rested with decreasing doses of IL-2 for 5 days.[17]

DNA methylation analysis by deep amplicon bisulphite sequencing

DNA isolation method, primer sequences and cycling conditions are included in supplementary material and methods and figure-MS1.

T-cell receptor diversity

Amplification and sequencing of [TCRB/IGH/IGKL/TCRAD/TCRG] CDR3 was performed using immunoSEQ Platform (Adaptive Biotechnologies, Seattle, WA), as previously described(supplementary methods). Power Geometric (PG) index with Horvitz-Thompson type was used as correction for under-sampling and Good-Turing coverage adjustment[18,19,20].

Gene expression

RNA extraction method is included in supplementary methods. Analysis of differential gene expression was performed as previously described[21,22](supplementary methods).

GEP data of this manuscript is deposited at gene expression omnibus(GEO), accession number: GSE78004

http://www.ncbi.nlm.nih.gov/geo/query/acc.cgi?token=qvclwscgnxgvtkz&acc=GSE78004

Statistical analysis

Different statistical methods have been used which are explained in the result section and/or figure legends. $P < 0.05$ was considered as statistically significant in all cases. Statistics were calculated using SPSS version 22 or R version 3.2.2.

Study approval

King's College Hospital Local Research Ethics Committee and Institutional Review Board of the National Heart, Lung, and Blood Institute (NIH) approved the clinical studies of IST and sample collection, and informed written consent was obtained from patients.

Results

Identification of an immune signature for AA compared to healthy individuals based on distinct Treg subpopulations

We analyzed 31 AA patients at diagnosis and 5 HDs. Of these 31 patients, 16 were part of an initial test cohort and a further 15 as validation cohort. Metal-tagged antibodies against surface and intra-cellular markers were used in 2 separate panels (with or without stimulation with PMA/Ionomycin) to stain T-cells, including known markers for Tregs (CD25, CD127, FOXP3), naïve/memory subsets, homing/trafficking receptors, and differentiation/activation markers (table-S1). $CD4^+$, $CD8^+$ T-cells and B cells were clustered using this "whole panel" clustering approach (34 markers in panel 1 (table S1)) to minimize bias. $FOXP3^+$ cells were also clustered within $CD4^+$ T-cells (figure-1 and figure-S1). After gating for $CD3^+$, $CD4^+$, $CD8^-$ and merging all samples, viSNE was performed and cells clustered, based on 13 markers which most clearly clustered Tregs (figures-2&S2). Treg subpopulations were clustered together and identified by high expression of CD25 and FOXP3 and low expression of CD127 (figure-2a and figure-S1b). Identified Tregs expressed $CD27^{hi}$, $CD45RA^{lo}$, $CD45RO^{hi}$, $CD95^{hi}$, $CD7^{lo}$, $CD28^{hi}$, $CCR4^{hi}$

compared to the total $CD4^+$ T-cell subpopulation (figure-2b). The frequency of total Tregs was significantly lower in AA patients compared to HDs (2.7 % v 5.7% of $CD4^+$ T-cells, *p<0.01*) confirming our previously published findings[8]. The numbers of Tregs were not significantly different between patients with severe (SAA)/ very severe AA(VSAA) and non-severe AA(NSAA).

Although viSNE clustered the Treg population in one area, density plots revealed a heterogeneous distribution of cells. Two subpopulations within Tregs with different frequency between AA and HDs were identified and designated as "Treg A" and "Treg B" (figure-2c&d and figure-S1b&c). To confirm the presence of these two subpopulations and eliminate any bias, dimensionality reduction and automated unsupervised clustering methodology was applied independently by the bioinformatician that confirmed the presence of two subpopulations within Tregs (figure-2c and figure-S1b&c). These two subpopulations showed distinct markers in AA Tregs (16 patients, 12 IST-responder and 4 non-responders) as well as 5 HDs. While both subpopulations were $CD25^{hi}$ and $FOXP3^{hi}$ and $CD127^{lo}$ compared to total $CD4^+$ T-cells, subpopulation B was additionally characterized by a lower expression of CD45RA (*p<0.0001*), CD7 (*p<0.001*), CD27 (p<0.05) and higher expression of CCR4 (*p<0.0001*), CCR6 (*p<0.0001*), CD25 (*p<0.0001*), CD28 (*p<0.01*), CD45RO (*p<0.0001*), CD95 (*p<0.0001*), CXCR3 (*p<0.05*), FOXP3 (*p<0.0001*) and HLA-DR (*p<0.0001*) compared to subpopulation A (Kruskal–Wallis one-way analysis of variance by ranks).

In addition to total Tregs, percentage of subpopulation B Tregs was significantly lower in AA patients compared to HDs(40.8%±13.7% v 72.2%±15, *p=0.008*).

Treg composition predicts response to IST at time of diagnosis of AA

When patients were stratified into IST-responders (n=12) and non-responders (n=4), while the overall frequency of Treg B was lower in both responder and non-responding patients at time of diagnosis compare to HDs (n=5) (48.8%±6.1 & 28.9%±2.7 v 72.2%±6.7, *p=0.005*, *p<0.0001*), non-responders had significantly higher Treg A and lower Treg B cells compared to responders (63.5%±4.5 v 38.8%±5.0, *p*<0.005 for Treg A, 28.9%±2.7 v 48.8%±6.1, *p*<0.05 for Treg B) (figure-2e and table-2).

To investigate the overlap between the Treg subpopulations with Treg subpopulations identified by Miyara et al[23], Tregs were gated based on CD45RA and FOXP3 expression. While subpopulation A and B mainly overlapped with subpopulations I ($CD45RA^{hi}$, $FOXP3^{lo}$) and II ($CD45RA^{lo}$, $FOXP3^{hi}$), respectively, subpopulation III ($CD45RA^{lo}$, $FOXP3^{lo}$) was spread over both population A and B area and some cells clustered outside Treg area(figure-2f).

Following IST response, the frequency of population A was significantly reduced in responders (from 38.8%±5.0 to 19.2%±2.4, *p<0.01*), but not significant in non-responder patients. Treg B frequency was significantly higher in responders compared to non-responders (59.9%±3.4 v 21.8%±4.3, *p*<0.0001) and closer to HDs (table-2). Treg population A or B were not significantly different between patients with severe/ very severe (n=11) and non-severe AA (n=5).

The cytokine profile of Tregs following stimulation with PMA, Ionomycin and Brefeldin-A was investigated. Treg subpopulations A and B were identified within Tregs (figure-S3). Stimulated Treg clusters expressed higher CD25 (*p<0.001*) and FOXP3 (*p=0.001*) and lower CD127 (*p=0.001*) compared to total $CD4^+$ T-cells. Majority of $CD4^+$ T-cells with pro-inflammatory cytokine properties clustered outside the "Treg area". Thus, Treg clusters expressed negligible amounts of pro-inflammatory cytokines IFN-γ, and IL-17 (figure-3a). Tregs expressed significantly higher IL-10 compared to total $CD4^+$ T-cells (*p=0.002*), however the IL-10 expression was not significantly different between the two Treg subpopulations. Although TNF-α expressing cells were clustered within non-Treg subpopulations, a cluster of $CD4^+$ TNF-α^+ T-cells clustered within Treg A subpopulation (figure-3b). These TNF-α^+ cells expressed significantly higher CD127 (*p<0.001*), and lower IL-10 (*p<0.001*), CD279 (*p<0.001*), HLA-DR (*p=0.003*), CD38 (*p<0.001*), CD25 (*p<0.001*) and FOXP3 (*p<0.001*) compared to total Tregs. Although at time of diagnosis the frequency of TNF-α^+ cells was not significantly different between IST responders and non-responders, IST responders had significantly lower TNF-α^+ cells compared to non-responder patients following response to IST (0.32% v 1.81%, *p=0.008*)(figure-3c).

Validation by conventional polychromatic flowcytometry

Conventional flow-cytometry was performed on PB from a separate validation cohort of 15 AA patients (11 IST responders and 4 non-responders) at time of diagnosis to confirm that the identified markers were sufficient to detect Treg subpopulations and whether the cytof -identified combination of markers was still predictive for IST response. PBMCs were stained with anti-CD4, CD25, CD127, FOXP3, CD95, CCR4 and CD45RA and similar to the initial cohort, Treg A were significantly higher in non-responders compared to responders (37.82%±5.11 v 18.33±2.31, *p*=0.006) whereas Treg B were significantly higher in responders (69.97%±3.02 v 49.34%±4.92, *p*=0.01)(figure-S4).

Conventional $CD4^+$ T-cells

Our marker panels also identified and clustered conventional $CD4^+$ T-cells (T_{con}). The Treg population was first gated out on viSNE plot and SPADE clustering based on CD45RA, CD45RO, CD27 and CD62L performed. T_{con} subpopulations were defined as naïve ($CD45RA^+$

CD45RO$^-$ CD27^{hi}), memory (CD45RA$^-$ CD45RO$^+$ CD27^{lo}), central memory (CD45RA$^-$ CD45RO$^+$ CD27^{lo} CD62L^{hi}), effector memory (CD45RA$^-$ CD45RO$^+$ CD27^{lo} CD62L^{lo}), effector (CD45RA$^-$ CD45RO$^+$ CD27^{lo}) and terminal effectors (CD45RA$^-$ CD45RO$^-$ CD27^{lo}).Subset frequencies were not significantly different between IST-responders (n=12) and non-responders (n=4) at time of diagnosis. However, effector CD4$^+$ T-cells (T_e) expressed significantly higher CD161 level in non-responders compared to responders ($p<0.01$) (figure-3d&e and table-S2).

Function, ontogeny and *in-vitro* expansion of Treg subsets

To assess function of the Treg subpopulations, HD CD4$^+$ Tregs were sorted based on CD25, CD127 and CD95 expression, that showed highest expression differences between subpopulation A and B on viSNE clusters, excluding intracellular markers to avoid fixation and permeabilisation of the cells. Sorted cells were CD4$^+$CD25^{hi} CD127^{lo} CD95$^-$, CD45RA^{hi}, CCR4^{lo} (subpopulation A) and CD4$^+$CD25^{hi} CD127^{lo} CD95$^+$, CD45RA^{lo}, CCR4^{hi} (subpopulation B). To confirm these markers were enough to identify Treg subpopulations, viSNE runs were performed based on the above markers and identified both subpopulations (figure-S5). Tregs B were significantly more functional compared to subpopulation A, in suppression of both IFN-γ and TNF-α secretion by T conventional ($p<0.05$, figure-4a).

Genomic DNA from sorted Tregs A and B was used for T-cell receptor (TCR) Vß chain complementarity determining regions (CDR3) high-throughput sequencing [19,20]. On average, subpopulation A and B had 33773 and 26090 unique TCR sequences, respectively, and 233 sequences were common to both (r=0.008) (figure-S6). T_{con} also shared 137 and 383 sequences with subpopulation A and B respectively (r=0.154 and r=0.092 respectively). It is recognized that in assessment of naturally, highly diverse TCR subpopulations, under-sampling can introduce bias[18 24]. We therefore used Power Geometric index (PG) for pairwise comparison of TCR repertoire overlap[18]. Overlap between Treg A, B and T_{con} was small suggesting these subpopulations were distinct (figure-4b).

Global gene expression (GEP) analysis of Treg subpopulations

Whole GEP data[25,26] showed both Treg A and Treg B had different GEP compared to $T_{con.}$ Nevertheless, when principle component analysis (PCA) was performed, Treg B and T_{con} had the highest difference while Treg A subpopulation showed a transcriptional profile in between Treg B and T_{con} (figure-S7).

Comparing GEPs of Treg subpopulations to T_{con}, using the human Treg's gene-signature, [27], showed both Treg A and B subpopulations were significantly enriched in genes up-regulated in human Tregs including: *IL-2RA, FOXP3, IKZF2, TIGIT and CTLA4* (*FDR*<0.0001 for both Treg subpopulations compared to T_{con}. Treg B cells were enriched with Treg-related memory/activation

genes compared to Treg A, - *JAKMIP1, CCR8, TRIB1* and *GZMK* (*FDR*<0.0001, figure-4c-e). Thus, while both Treg subpopulations were enriched with Treg associated genes, Tregs B were characterized by an activation gene signature in agreement with mass-cytometry findings.

Gene set enrichment (GSEA) functional analysis[22] highlighted several genesets as significantly overexpressed in Treg B subpopulation including: G2M checkpoint (FDR<0.0001), mitosis (FDR=0.015), M phase of mitotic cell-cycle (FDR=0.018) IL2-STAT5 signaling (FDR=0.023) and immune response genes (FDR=0.032) (table-3). Protein interaction networks of proteins encoded by mRNA that are enriched in Treg B subpopulation were also mapped (see supplement and figures S8a&b). Ontology analyses of the functions of these protein complexes (table-S3 and figure-S9) showed they are involved in mitotic functions, DNA replication and cell-cycle-dependent transcription. MKI67 mRNA (encodes nuclear Ki67 protein) was enriched in Treg B subpopulation. This is important as Ki67 protein is often used as a marker of proliferating cells [28,29].

Expandability of Tregs in Treg promoting culture

One of the aims of this study was to investigate the potential expandability of Tregs in AA. We first tested the IL-2 sensitivity of AA total Tregs based on STAT5 phosphorylation.[30] Freshly isolated PBMCs from two HDs and six AA patients (3 IST-responders and 3 non-responders, at diagnosis) were cultured in the presence of IL-2 at different concentrations (from 0.1 to 1000 IU/ml). Treg p-STAT5 expression significantly increased after 15 minutes culture with IL-2 (0.5 IU/mL) (median fluorescence intensities (MFI) 92.6±35.1 pre IL-2 versus 787±109.6 post IL-2, *p < 0.001)* confirming their responsiveness to IL-2. There was no difference between HDs and AA Tregs in response to IL-2 (figure-5a).

To test their *in-vitro* expandability, Tregs were obtained from 6 AA patients (3 IST-responders and 3 non-responders, at diagnosis) and 8 HDs and were cultured and stimulated with anti CD3/CD28 beads (1:1 ratio) and high dose IL-2 (1,000 IU/mL) for four weeks with added all-trans retinoic acid 2 μM and rapamycin 100 nM.[17] AA Tregs expanded in a comparable rate to HD Tregs, with median 33 fold increase (range 29-149) compared to 21 fold increase (range 8-36) in HD. Expanded Tregs demonstrated more than 90% $FOXP3^+$ expression in both AA and HDs (figure-5 b&c).

Expanded Tregs were gradually (within 5 days) deprived of IL-2 following expansion and p-STAT5 evaluated in both AA and HDs Tregs to assess IL-2 dependency. Although expanded AA Tregs showed slightly lower p-STAT5 level following IL-2 deprivation, they responded to low dose IL-2 and p-STAT5 and returned to a similar level as in HDs(data not shown).

Expanded Tregs function, methylation status of TSDR and TCR diversity

To assess the suppressive activity of expanded Tregs, T_{con} were stained with a fluorescent proliferation dye (CellTrace Violet, Life Technologies) and co-cultured with autologous expanded Tregs (1:1 ratio) for 5 days in the presence of anti CD3/CD28 beads (T_{con}:Treg:beads=20:20:1). Expanded AATregs suppressed proliferation of $CD4^+$ T_{con} (an average reduction from 43% to 5%, $p = 0.009$) in both autologous and allogeneic conditions(figure-5d). The suppressive activity of AA expanded Tregs was not significantly different from HD expanded Tregs.

To assess stability of expanded Tregs, we investigated the methylation status of 15 CpG sites within the *FOXP3 Treg-specific demethylated region* (TSDR)[31] by amplicon sequencing of bisulfite treated DNA on an Illumina MiSeq sequencing platform. TSDR CpG sites in expanded HDs and AA Tregs were >98% unmethylated, confirming stability of expanded Tregs(figure-6a).

TCR Vß CDR3 high-throughput sequencing of expanded Tregs was used to investigate their clonality. The normalized Shannon entropy of expanded Treg repertoire was used to calculate the degree of clonality which on average was 0.12 (four expanded Tregs, 1 being the most clonal and 0 the most TCR diversity). Both AA and HDs expanded Tregs showed a comparable level of TCR Vß CDR3 diversity, as defined (methods S)(figure-6b).

The (dis)similarity of *in-vitro* expanded Tregs with Treg A and Treg B was next investigated. As the isolated Tregs were stimulated and treated in a Treg skewing environment, the expression level of some markers like CD25 or FOXP3 were high in expanded Tregs, making it difficult to cluster expanded Tregs with Treg A or B of untouched Tregs for comparison. To overcome this technical issue, we used an alternative analysis approach based on distance calculation and relative expression of markers. Subpopulation of Tregs expanded *in-vitro* were assessed using the Euclidian distance between the mean expression for each parameter in Treg A and B (figure-6c and S10).

Using a one tail Welch Two Sample t-test we rejected the null hypothesis that the distance between Treg A and expanded Tregs is lower than Treg B ($p<2.2 \times 10^{-16}$), suggesting that expanded Tregs were more similar to subpopulation B than A.

Discussion

Although the importance of Tregs in the pathophysiology of autoimmune diseases is well established, the definition and significance of Treg subpopulations is less clear. Identification of Treg subsets is challenging in autoimmune diseases as the number of Tregs is usually low and Tregs may express aberrant markers, and gating strategies for Treg subpopulations are often subjective. Biomarkers that, first, identify AA patients from HDs and, second, identify at time of

diagnosis who are less likely to respond to IST, have as yet not been identified. It is now possible to comprehensively characterize rare, complex populations of cells with minimal bias[15,32] using mass-cytometry (CyTOF) to measure the expression level of more than 40 parameters at the single cell level[32,33,34]. The complexity of Treg subsets in HDs has been previously demonstrated by mass-cytometry on sorted Tregs[35], however, their biological importance has not been investigated. In current study, by using this multidimensional phenotyping and unbiased approach, two distinct Treg subpopulations were characterized in HDs and AA patients and the changes in these subsets predicted response to IST at diagnosis of AA. We sorted these cells based on their immunological markers and confirmed their dissimilar TCR, gene expression signatures and function. Our analytical strategy eliminated the unavoidable subjectivity of Treg subpopulation definition based on two-dimensional gating without unnecessary over-clustering.

Within the $CD25^{hi}$, $FOXP3^{hi}$ and $CD127^{lo}$ Treg population, AA Tregs expressed $CD27^{hi}$, $CD45RA^{lo}$, $CD45RO^{hi}$, $CD95^{hi}$, $CD7^{lo}$, $CD28^{hi}$, $CCR4^{hi}$ compared to the total $CD4^{+}$ T-cell. We have identified two well-defined subpopulations within this Treg population, ('Treg A and B'). While total Treg numbers were reduced in AA, Treg A was significantly higher in AA patients compared to HDs. In contrast, the number of Treg B subpopulation was significantly lower in AA patients compared to HDs (table 2). Subpopulation B was characterized by a lower expression of CD45RA, CD7, CD27 and higher expression of CCR4, CCR6, CD25, CD28, CD45RO, CD95, CXCR3, FOXP3 and HLA-DR. The most significantly different markers were CD95, CCR4 and CD45RO[36-38]. The identified Treg subpopulations were compared to established Treg subpopulation definitions[23]. While Treg A and B overlap with Treg subpopulations I and II respectively, our approach demarcates those Treg III cells which are closer to Tregs and combine them with subpopulation A or B based on their phenotype and eliminate cells which are closer to T_{con} and less likely to be regulatory. There is an unmet need for more robust predictive factors for response to IST at time of diagnosis of AA. Known predictive factors for response to IST include less severe disease, young age, and absolute reticulocyte and lymphocyte counts of ≥ 25 and $\geq 1.0 \times 10^9$/l, respectively [39]. Short telomeres in children, but not in adults, also predict response to IST [40,41]. The presence of a *PIGA* mutation predicts for response to IST, as does a somatic *BCOR/BCORL* mutation. In contrast, somatic mutation of *DNMT3A* or *ASXL1* is associated with worse outcomes following IST[42]. We have identified an immune signature that predicts for response to IST for an individual patient at time of diagnosis of AA. Non-responders to IST were more likely to have higher Treg A compared to non-responders, whereas responders had higher Treg B numbers compared to HDs(figure-7). Treg B subpopulation characterized by a more "activated/memory" phenotype. We also tested this combination of identified markers in a

separate validation cohort of AA patients, using conventional flow-cytometry, and confirmed the predictive value of this combination for response to IST.

To explore the potential therapeutic application of expanded Tregs in the treatment of AA, we examined the characteristics and in vitro expandability of the Treg subpopulations in depth. Both AA and HDs Tregs were sensitive to IL-2 as assessed by STAT5 phosphorylation. The expansion rate of AA Tregs (three of them from IST non-responders) was not different from HDs after 4 weeks culture. Expanded Tregs were functional in both autologous and allogeneic settings, and TSDR of expanded Tregs indicated a stable phenotype. Treg B population was more functional in suppressing IFN-γ and TNF-α secretion by T_{con} compared to Treg A cells. Although both Treg subpopulations were significantly enriched with Treg specific genes such as *IL-2RA, FOXP3, IKZF2, TIGIT and CTLA4* compared to T_{con}, nevertheless, TCR sequence overlaps between Treg A, Treg B and T_{con} were minimal, suggesting possible distinct developmental origins. Functional GEP analysis revealed marked enrichment of Treg B subpopulation with G2M checkpoint and mitosis related genes suggesting that Tregs B are more prone to enter cell-cycle. In studies of human primary lymphocytes and $CD34^+$ cells, we showed that quiescent (G_0) cells do not contain many proteins required for cell proliferation (*e.g.* DNA synthesis and mitosis) or molecules that regulate cell-cycle [43-45] [46,47]. Expression of mRNA encoding proteins involved in mitosis, DNA replication and other proliferation functions suggest that the Treg B subpopulation is more likely to be proliferating, primed to proliferate or they have recently exited the cell-cycle. The limitation of this study was the very low number of Tregs in AA patients, which made it technically difficult to individually assess the IL-2 sensitivity and *in-vitro* expandability of patient's Treg subpopulations. Nonetheless, the observation that IST-responder patients had a significantly higher frequency of Treg B following IST therapy compared to IST non-responders would support the hypothesis that Treg B are more likely to proliferate and perhaps better control the immune response in AA, particularly following treatments with ATG-based immunosuppressive therapy, when the number of T cells are reduced and the ability of Tregs to proliferate would be crucial to reinstate a balanced immune-response (figure 7).

In-vitro expansion of Tregs for clinical use is an emerging cellular therapy in GVHD, type-I diabetes and organ transplant rejection.[48-52] Nevertheless, the quality control of expanded Tregs is a time consuming procedure. Our data comparing expanded Tregs with pre-expansion Treg subpopulations could provide a robust and quick screening for quality control of cell therapy products, and may serve as a predictive tool for expandability of Tregs in AA and other autoimmune diseases.

In summary, we have shown for the first time that a novel strategy for multidimensional deep-phenotyping can reliably identify an immune signature for AA based on Treg subpopulations. This approach also identifies an immune signature that predicts for response to IST at time of diagnosis of AA, and which may allow a more patient specific approach to future treatment decision-making in SAA. Our findings also pave the way for future novel therapeutic approaches such as expanded autologous Tregs and low dose interleukin-2 in AA.

Conflict of interest disclosure

JMI is co-founder and board member at Cytobank Inc.

Acknowledgments

This work is supported by a research program grant from Bloodwise, UK and a grant from UK&MDSIF, USA. We would like to thank King's College London Genomic Centre for performing gene expression experiments in particular Dr Matthew Arno. We also thank the Hematology department tissue bank for processing patient samples. We are grateful to Professor Giovanna Lombardi, Dr Cristiano Scotta, Dr Behdad Afzali and Professor Claudia Kemper for their scientific input. The authors acknowledge financial support from the Department of Health via the National Institute for Health Research (NIHR) comprehensive Biomedical Research Centre award to Guy's & St Thomas' NHS Foundation Trust in partnership with King's College London and King's College Hospital NHS Foundation Trust.

Author contributions

SK: Designed, supervised and performed experiments, analyzed and interpreted data, wrote the paper, BC: Designed and performed experiments, analyzed and interpreted data, wrote the paper, TS: Design and perform experiments, analyzed and interpreted data, wrote paper, PPA: Validated metal tagged antibodies, MML: Analyzed and interpreted GEP data, contributed in writing the paper, DM: provided clinical data and contributed in writing the paper, KD: Contributed in data analysis, AK: provided clinical data, CB: Performed experiments, XF: Provided clinical samples and data, AS: Analyzed data, SM: Performed experiments, RM: Bioinformatics and statistical analysis, EDR: Supervised bioinformatics and statistical analysis, SH, Mass-cytometry data quality control and contributed in writing the paper, RE: Mass-cytometry data acquisition and quality control, NP: Bioinformatics and statistical analysis, GAMP: GEP data analysis, NSBT:

Cell-cycle related data analysis and contributed in writing the paper, FF: contributed in writing the paper, JMI: Contributed in data analysis, interpreting data and contributed in writing the paper, NY: Provided clinical samples and data, contributed in writing the paper, JCWM: Provided clinical samples and data, supervised the project, interpreted the results and contributed in writing the paper, GJM: Supervised the project, interpreted the results and wrote the paper.

References

1. Olnes MJ, Scheinberg P, Calvo KR, et al. Eltrombopag and improved hematopoiesis in refractory aplastic anemia. *N Engl J Med*. 2012;367(1):11-19.
2. Desmond R, Townsley DM, Dumitriu B, et al. Eltrombopag restores trilineage hematopoiesis in refractory severe aplastic anemia that can be sustained on discontinuation of drug. *Blood*. 2014;123(12):1818-1825.
3. Scheinberg P, Young NS. How I treat acquired aplastic anemia. *Blood*. 2012;120(6):1185-1196.
4. Marsh JC, Bacigalupo A, Schrezenmeier H, et al. Prospective study of rabbit antithymocyte globulin and cyclosporine for aplastic anemia from the EBMT Severe Aplastic Anaemia Working Party. *Blood*. 2012;119(23):5391-5396.
5. Passweg JR, Marsh JC. Aplastic anemia: first-line treatment by immunosuppression and sibling marrow transplantation. *Hematology Am Soc Hematol Educ Program*. 2010;2010:36-42.
6. Young NS, Bacigalupo A, Marsh JC. Aplastic anemia: pathophysiology and treatment. *Biol Blood Marrow Transplant*. 2010;16(1 Suppl):S119-125.
7. Kulasekararaj AG, Jiang J, Smith AE, et al. Somatic mutations identify a subgroup of aplastic anemia patients who progress to myelodysplastic syndrome. *Blood*. 2014;124(17):2698-2704.
8. Kordasti S, Marsh J, Al-Khan S, et al. Functional characterization of CD4+ T cells in aplastic anemia. *Blood*. 2012;119(9):2033-2043.
9. Solomou EE, Rezvani K, Mielke S, et al. Deficient CD4+ CD25+ FOXP3+ T regulatory cells in acquired aplastic anemia. *Blood*. 2007;110(5):1603-1606.
10. Chen J, Ellison FM, Eckhaus MA, et al. Minor antigen h60-mediated aplastic anemia is ameliorated by immunosuppression and the infusion of regulatory T cells. *J Immunol*. 2007;178(7):4159-4168.
11. Shi J, Ge M, Lu S, et al. Intrinsic impairment of CD4(+)CD25(+) regulatory T cells in acquired aplastic anemia. *Blood*. 2012;120(8):1624-1632.
12. van der Maaten L. Visualizing Data using t-SNE. *Journal of Machine Learning Research*. 2008;9: 2579-2605
13. Amir el AD, Davis KL, Tadmor MD, et al. viSNE enables visualization of high dimensional single-cell data and reveals phenotypic heterogeneity of leukemia. *Nat Biotechnol*. 2013;31(6):545-552.
14. Qiu P, Simonds EF, Bendall SC, et al. Extracting a cellular hierarchy from high-dimensional cytometry data with SPADE. *Nat Biotechnol*. 2011;29(10):886-891.
15. Diggins KE, Ferrell PB, Jr., Irish JM. Methods for discovery and characterization of cell subsets in high dimensional mass cytometry data. *Methods*. 2015;82:55-63.
16. Kotecha N, Krutzik PO, Irish JM. Web-based analysis and publication of flow cytometry experiments. *Curr Protoc Cytom*. 2010;Chapter 10:Unit10 17.
17. Scotta C, Esposito M, Fazekasova H, et al. Differential effects of rapamycin and retinoic acid on expansion, stability and suppressive qualities of human CD4(+)CD25(+)FOXP3(+) T regulatory cell subpopulations. *Haematologica*. 2013;98(8):1291-1299.
18. Rempala GA, Seweryn M. Methods for diversity and overlap analysis in T-cell receptor populations. *J Math Biol*. 2013;67(6-7):1339-1368.
19. Robins HS, Campregher PV, Srivastava SK, et al. Comprehensive assessment of T-cell receptor beta-chain diversity in alphabeta T cells. *Blood*. 2009;114(19):4099-4107.
20. Carlson CS, Emerson RO, Sherwood AM, et al. Using synthetic templates to design an unbiased multiplex PCR assay. *Nat Commun*. 2013;4:2680.
21. Mootha VK, Lindgren CM, Eriksson KF, et al. PGC-1alpha-responsive genes involved in oxidative phosphorylation are coordinately downregulated in human diabetes. *Nat Genet*. 2003;34(3):267-273.
22. Subramanian A, Tamayo P, Mootha VK, et al. Gene set enrichment analysis: a knowledge-based approach for interpreting genome-wide expression profiles. *Proc Natl Acad Sci U S A*. 2005;102(43):15545-15550.
23. Miyara M, Yoshioka Y, Kitoh A, et al. Functional delineation and differentiation dynamics of human CD4+ T cells expressing the FoxP3 transcription factor. *Immunity*. 2009;30(6):899-911.
24. Venturi V, Kedzierska K, Tanaka MM, Turner SJ, Doherty PC, Davenport MP. Method for assessing the similarity between subsets of the T cell receptor repertoire. *J Immunol Methods*. 2008;329(1-2):67-80.
25. Mohamedali A, Gaken J, Twine NA, et al. Prevalence and prognostic significance of allelic imbalance by single-nucleotide polymorphism analysis in low-risk myelodysplastic syndromes. *Blood*. 2007;110(9):3365-3373.
26. Mold JE, Venkatasubrahmanyam S, Burt TD, et al. Fetal and adult hematopoietic stem cells give rise to distinct T cell lineages in humans. *Science*. 2010;330(6011):1695-1699.
27. Ferraro A, D'Alise AM, Raj T, et al. Interindividual variation in human T regulatory cells. *Proc Natl Acad Sci U S A*. 2014;111(12):E1111-1120.
28. Viale G. Pathological work up of the primary tumor: getting the proper information out of it. *Breast*. 2011;20 Suppl 3:S82-86.

29. Hsi ED, Jung SH, Lai R, et al. Ki67 and PIM1 expression predict outcome in mantle cell lymphoma treated with high dose therapy, stem cell transplantation and rituximab: a Cancer and Leukemia Group B 59909 correlative science study. *Leukemia & lymphoma*. 2008;49(11):2081-2090.
30. Mahmud SA, Manlove LS, Farrar MA. Interleukin-2 and STAT5 in regulatory T cell development and function. *JAKSTAT*. 2013;2(1):e23154.
31. Toker A, Engelbert D, Garg G, et al. Active demethylation of the Foxp3 locus leads to the generation of stable regulatory T cells within the thymus. *J Immunol*. 2013;190(7):3180-3188.
32. Irish JM. Beyond the age of cellular discovery. *Nat Immunol*. 2014;15(12):1095-1097.
33. Newell EW, Sigal N, Bendall SC, Nolan GP, Davis MM. Cytometry by time-of-flight shows combinatorial cytokine expression and virus-specific cell niches within a continuum of CD8+ T cell phenotypes. *Immunity*. 2012;36(1):142-152.
34. Wong MT, Chen J, Narayanan S, et al. Mapping the Diversity of Follicular Helper T Cells in Human Blood and Tonsils Using High-Dimensional Mass Cytometry Analysis. *Cell Rep*. 2015;11(11):1822-1833.
35. Mason GM, Lowe K, Melchiotti R, et al. Phenotypic Complexity of the Human Regulatory T Cell Compartment Revealed by Mass Cytometry. *J Immunol*. 2015;195(5):2030-2037.
36. Weiss EM, Schmidt A, Vobis D, et al. Foxp3-mediated suppression of CD95L expression confers resistance to activation-induced cell death in regulatory T cells. *J Immunol*. 2011;187(4):1684-1691.
37. Kanakry CG, Ganguly S, Zahurak M, et al. Aldehyde dehydrogenase expression drives human regulatory T cell resistance to posttransplantation cyclophosphamide. *Sci Transl Med*. 2013;5(211):211ra157.
38. Baatar D, Olkhanud P, Sumitomo K, Taub D, Gress R, Biragyn A. Human peripheral blood T regulatory cells (Tregs), functionally primed CCR4+ Tregs and unprimed CCR4- Tregs, regulate effector T cells using FasL. *J Immunol*. 2007;178(8):4891-4900.
39. Scheinberg P, Wu CO, Nunez O, Young NS. Predicting response to immunosuppressive therapy and survival in severe aplastic anaemia. *Br J Haematol*. 2009;144(2):206-216.
40. Narita A, Muramatsu H, Sekiya Y, et al. Paroxysmal nocturnal hemoglobinuria and telomere length predicts response to immunosuppressive therapy in pediatric aplastic anemia. *Haematologica*. 2015;100(12):1546-1552.
41. Scheinberg P, Cooper JN, Sloand EM, Wu CO, Calado RT, Young NS. Association of telomere length of peripheral blood leukocytes with hematopoietic relapse, malignant transformation, and survival in severe aplastic anemia. *JAMA*. 2010;304(12):1358-1364.
42. Yoshizato T, Dumitriu B, Hosokawa K, et al. Somatic Mutations and Clonal Hematopoiesis in Aplastic Anemia. *N Engl J Med*. 2015;373(1):35-47.
43. Williams CD, Linch DC, Watts MJ, Thomas NS. Characterization of cell-cycle status and E2F complexes in mobilized CD34+ cells before and after cytokine stimulation. *Blood*. 1997;90(1):194-203.
44. Lea NC, Orr, S. J., Stoeber, K., Williams, G. H., Lam, E. W. -F., Ibrahim, M. A. A., Mufti, G. J. and Thomas, N. S. B. Commitment point during G0->G1 that controls entry into the cell-cycle. *Mol Cell Biol*. 2003;23(7):2351-2361.
45. Lea NC, Thomas, N. S. B. Cell-cycle proteins. In: Hughes D, Mehmet, H., ed. Cell Proliferation and Apoptosis. Oxford: Bios Scientific Publishers; 2003:77-122.
46. Thomas NSB. Cell-cycle regulation. In: Degos L, Griffin, J. D., Linch, D. C. and Lowenberg, B., ed. Textbook of Malignant Haematology. London: Martin Dunitz; 2004:33-63.
47. Orr SJ, Gaymes T, Ladon D, et al. Reducing MCM levels in human primary T cells during the G(0)-->G(1) transition causes genomic instability during the first cell-cycle. *Oncogene*. 2010;29(26):3803-3814.
48. Brunstein CG, Miller JS, Cao Q, et al. Infusion of ex vivo expanded T regulatory cells in adults transplanted with umbilical cord blood: safety profile and detection kinetics. *Blood*. 2011;117(3):1061-1070.
49. Hoffmann P, Eder R, Kunz-Schughart LA, Andreesen R, Edinger M. Large-scale in vitro expansion of polyclonal human CD4(+)CD25high regulatory T cells. *Blood*. 2004;104(3):895-903.
50. Bluestone JA, Trotta E, Xu D. The therapeutic potential of regulatory T cells for the treatment of autoimmune disease. *Expert Opin Ther Targets*. 2015;19(8):1091-1103.
51. Putnam AL, Safinia N, Medvec A, et al. Clinical grade manufacturing of human alloantigen-reactive regulatory T cells for use in transplantation. *Am J Transplant*. 2013;13(11):3010-3020.
52. Bluestone JA, Buckner JH, Fitch M, et al. Type 1 diabetes immunotherapy using polyclonal regulatory T cells. *Sci Transl Med*. 2015;7(315):315ra189.

Tables

Characteristic	Value
Number of patients	39
Median age, y (range)	45 (20-72)
Gender	
M	19
F	20
Disease severity at diagnosis	
VSAA	11
SAA	16
NSAA	12
PNH clone at the time of study	
Yes	28
No	11
Size of PNH clone, % (range)	
Red cells	0.402 (0-87.3)
Granulocytes	3.86 (0-96.7)
Monocytes	4.517 (0-91.8)
Etiology	
Idiopathic	39
Response to treatment	
CR	6
PR	19
NR	14

y: years, M: male, F: female, VSAA: very severe aplastic anaemia, SAA: severe aplastic anaemia, NSAA: non-severe aplastic anaemia, PNH: paroxysmal nocturnal haemoglobinuria, CR: complete response, PR: partial response, NR: non-response

Table 1. Patients' characteristics: Thirty-nine AA patients were recruited in this study and PB samples were used for mass-cytometry and/or *in-vitro* experiments. AA patients who were eligible for IST were randomly selected and invited to participate in this study. A small to moderate PNH clone was detected in 28 patients, with no cases of hemolytic PNH.

Peripheral blood mononuclear cells (PBMCs) from 16 patients (12 IST responder and 4 non-responders) were used for initial CyTOF analysis and samples from another 15 patients (11 IST responders and 4 non-responders) were used as validation cohort. PBMCs from additional 8 patients were used for functional assays. Among non responder patients (n=14), 7 patients were transplanted later on and the remaining were treated with CsA and supportive care.

Treg subpopulation	Markers	Healthy Donors	IST responder AA pre-treatment	IST non-responder AA pre-treatment	IST responder AA post-treatment	IST non-responder AA post-treatment
Treg A	CD45RA↑ CD7↑ CD27↑ CCR4↓ CCR6↓ CD25*↓ CD28↓ CD45RO↓CD95↓ CXCR3↓ FOXP3*↓ HLA-DR↓	Minor population 20.3%±6.5	↑ 38.8%±5.0	↑↑ 63.5%±4.5	↓ 19.26%±2.43	NSC 73.9%±6.8
Treg A (TNF-α +)	TNF-a + IL-10↓ CD279↓ HLA-DR↓ CD38↓	R 1.2%±0.3	NSC 0.75%±0.14	NSC 0.79%±0.13	↓0.32%±0.12	NSC 1.81%±0.19
Treg B	CD45RA↓ CD7↓ CD27↓ CCR4↑ CCR6↑ CD25‡↑ CD28↑ CD45RO↑CD95↑ CXCR3↑ FOXP3‡↑ HLA-DR↑	Major population 72.2%±6.7	↓ 48.8%±6.1	↓↓ 28.9%±2.7	↑59.98%±3.18 NS	NSC 21.8%±4.3

Table 2. Treg A and B markers and summary of changes in AA: Surface and intracellular markers which are significantly higher or lower in Treg subpopulations as well as their frequencies in healthy donors, IST responder and non-responder AA patients prior and after IST.

*Lower expression compared to Treg B subpopulation.

‡Higher expression compared to Treg A subpopulation.

R: reference value, NSC: no significant change

Geneset	FDR q-value	Normalized Enrichment Score (NES)	Significant genes
G2M checkpoint	<0.0001	2.0188198	*CASC5, NUSAP1, CENPE, TPX2, TOP2A, KIF11, BARD1, EZH2, SLC7A5, HN1, GINS2, CKS2, BUB1, SMC4, STIL, BRCA2, CHEK1, SAP30, E2F3, MKI67, CDKN2C, NEK2, KIF15, KPNA2, KIF23, ZAK, POLQ, WHSC1, TFDP1, UCK2, E2F2, CDKN3, CDC7, E2F1, AURKA, CDC20, EFNA5, KIF4A, EXO1, CDC25A , PRC1, KIF5B*
Mitosis	0.014934987	2.020	*NCAPH, NUSAP1, NDC80, CENPE, BUB1B, TPX2, KIF11, TTN, BUB1, NEK2, SMC4, PCBP4, PAM*
M phase of mitotic cell cycle	0.01755665	2.0006573	*NCAPH, NUSAP1, NDC80, CENPE, BUB1B, TPX2, KIF11, TTN, BUB1, NEK2, SMC4, PCBP4, PAM*
IL2-STAT5 signalling	0.02301426	1.5519865	*SYT11, CCR4, TNFRSF9, CST7, ADAM19, IL1R2, ANXA4, PHLDA1, SLC1A5, IL18R1, FGL2, TNFRSF18, TNFRSF4, GALM, CXCL10, BATF, SPP1, TNFSF10, PHTF2, CD86, AHNAK, IL10, LIF, TLR7, F2RL2, CD79B, CTLA4, FURIN, TNFRSF1B, CAPG, ALCAM, CSF1, CASP3, CSF2, MUC1, MYO1E RORA, ITGAV, PRNP, ICOS, UCK2, CYFIP1, SOCS1*
Immune response genes	0.031976275	1.9183398	*IL7, CCR2, CCR8, CCR4, IL1R2, CCR6, CST7, CCL20, GZMA, CADM1, AIM2, CIITA, CCR5, CTSC, IL12A, NCF4, IL4, CCR9, GEM, IL32, TNFRSF4, LAX1, DEFB4A , FCGR3B, TLR7, CD74, APOA4, CCL5, APOBEC3G, CD79B, CTLA4*

Table 3. Genesets which are upregulated in Treg population B compared to population A: The most significant genesets which are up-regulated in Treg B subpopulation compared to Treg A are listed in this table. Leading edge analysis revealed several genes that significantly contribute in each genesets and enriched in Treg B compared to Treg A (marked as significant genes).

.

Figure legends

Figure 1. Peripheral blood mononuclear cell staining and clustering: PBMCs from AA and HDs were clustered using 34 surface and intracellular markers as our panel 1 (table S1). Intact cells were gated based on Ir-191 and event length, followed by Ir-191 and Ir-193 gating. Viable cells were selected based on CD45 expression and negativity for Rh. All FCS files were first normalized using control beads and analyzed using Cytobank web-based software (see the material and methods). $CD4^+$, $CD8^+$ T cells and B cells clustered together in both aplastic anemia (AA) and healthy donor (HD). Figures are representatives of 16 AA and 5 HDs samples.

Figure 2. Identification of Treg subset by automated clustering.

A) After initial gating for $CD3^+$, $CD4^+$ and $CD8^-$ T cells, the gated cells were clustered using viSNE (Cytobank). Treg population was identified based on high expression of CD25 and FOXP3 and low CD127 expression.

B) Median expression of the 7 most discriminative parameters between Total CD4+ cells and Tregs as identified by the automated clustering algorithm FLOCK on a subset of 700,000 cells proportionally selected from all samples. Tregs were defined as clusters whose median expression was simultaneously higher than the 90% quantile of FOXP3 expression, higher than the 90% quantile of CD25 expression and lower than the 50% quantile of CD127 expression across all $CD3^+CD8^-$ cells. Heatmap plot is based on 19 AA samples (pre and post IST) and 5 HDs samples.

C) Median expression of the 8 most discriminative parameters between the two subpopulations of Tregs identified by the automated clustering algorithm FLOCK. Expression values were asinh-transformed using a cofactor of 5. Heatmap plot is based on 19 AA samples (pre and post IST) and 5 HDs samples.

D) The density plot of viSNE plots revealed 2 subpopulations within Tregs, designated as Treg A and B (arrows). The frequencies of Treg A and B were different between healthy donors (HDs) and AA patients. Patients who did not respond to immunosuppressive therapy (IST NR) had higher number of Treg A at time of diagnosis compared to responder patients (IST R) and HDs.

The right viSNe plots are overlay of Tregs' contour plots colored by density and $CD4^+$ T cells uncolored contour plots.

E) At time of diagnosis and prior to treatment, Treg A frequency was higher in responder as well as non-responder patients compare to HDs (38.8%±5 & 63.5%±4.5 v 20.3%±6.6, $p<0.05$, $p<0.0001$). Whereas the frequency of Treg B was lower in both responder and non-responder AA patients at time of diagnosis compare to HDs (48.8%±6.1 & 28.9%±2.7 v 72.2%±6.7, $p=0.005$, $p<0.0001$). The non-responder patients however, had significantly higher Treg A and lower Treg B compared to responder patients (63.5%±4.5 v 38.8%±5.0, $p<0.005$ for Treg A, 28.9%±2.7 v

48.8%±6.1, $p<0.05$ for Treg B). Error bars are standard error of mean. Kruskal–Wallis one-way ANOVA test was used for statistical analysis.

****** $p<0.0001$, *** $p<0.001$, ** $p<0.01$, * $p<0.05$**

F) The overlap between the Treg subpopulations which were identified using viSNE and manually gated Treg populations based on CD45RA and FOXP3 expression. While subpopulation A and B mainly overlap with subpopulations I ($CD45RA^{hi}$, $FOXP3^{lo}$) and II ($CD45RA^{lo}$, $FOXP3^{hi}$) respectively, subpopulation III ($CD45RA^{lo}$, $FOXP3^{lo}$) was spread over population B as well as outside Treg area.

Figures are overlay of manually gated Treg populations on viSNE plot of total $CD4^+$ T cells from an IST responder AA patient.

Figure 3. PMA/Ionomycin stimulated Treg and T_{con} subpopulations: PBMCs from 16 patients and 5 HDs were stimulated for 4 hours with PMA (Phorbol 12-Myristate 13-Acetate) and a calcium ionophore (Ionomycin) and the protein transport inhibitor (Brefeldin A) and stained with a panel of antibodies based on 29 surface markers, transcription factors and cytokines (table 1s). Treg subpopulations A and B were identified within Tregs after stimulation with Treg profiles that distinguished responders from non-responders to IST (figure S3).

A) Following 4 hours stimulation with PMA and ionomycin in the presence of brefeldin, PBMCs were stained for surface and intracellular markers (supplementary table 1, panel 2) followed by mass-cytometry and viSNE on $CD4^+$ T cells. Cytokine secreting $CD4^+$ T cells including IFN-ϒ, IL-2, IL-17 and IL-4 secreting cells localized distinctly with minimal overlap and outside "Treg's area". Both Treg A and Treg B populations show higher expression of IL-10 compared to "non-Tregs" and TNF-α secreting Tregs but there was no significant difference between Tregs A and Treg B in terms of IL-10 expression.

B) Unlike the rest of cytokine secreting $CD4^+$ T cells, TNF-α secreting cells were spread over several areas including Treg A subpopulation (red arrow).

C) Spanning-tree progression analysis of density-normalized events (SPADE) analysis of Treg A and B following 4 hours stimulation with PMA/Ionomycin stimulation and intracellular staining (supplementary table 1, panel 2). While the TNF-α secreting cells within Treg A subpopulation reduces following IST in responder AA patients, there is no similar reduction in non-responder patients (patient AA-11 is an IST non-responder and AA-6 is a responder patient).

D & E) SPADE clustering based on CD45RA, CD45RO, CD27 and CD62L. The T_{con} subpopulations were defined as naïve ($CD45RA^+$ $CD45RO^-$ $CD27^{hi}$), memory ($CD45RA^-$ $CD45RO^+$ $CD27^{lo}$), central memory ($CD45RA^-$ $CD45RO^+$ $CD27^{lo}$ $CD62L^{hi}$), effector memory

(CD45RA$^-$ CD45RO$^+$ CD27^{lo} CD62L^{lo}), effector (CD45RA$^-$ CD45RO$^+$ CD27^{lo}) and terminal effectors (CD45RA$^-$ CD45RO$^-$ CD27^{lo}). Tcon with effector phenotype express higher CD161 in non-responder patients at time of diagnosis compared to responder AA patients. (patient AA-11 is an IST non-responder and AA-6 is a responder patient). The frequencies of these subpopulations were not significantly different between IST responder and IST non-responder patients at time of diagnosis. The naïve Tcon from IST non-responder patients were expressing slightly higher CCR4 compared to responder patients (see table s2).

Figure 4. Function and ontogeny of Treg subpopulations

A) Suppression of Tcon cytokine secretion by Treg subpopulations: CD4$^+$CD25^{hi} CD127^{lo} CD45-RA^{hi}, CD95$^-$, CCR4^{lo} (subpopulation A), CD4$^+$CD25^{hi} CD127^{lo} CD45-RA^{lo} CD95$^+$ CCR4^{hi} (subpopulation B) and CD4$^+$CD25^{low} T_{con} were sorted (FacsAria) and cultured for five days with anti CD3/CD28 beads (Tcon:Treg:bead = 20:20:1). After five days of culture, the supernatant was analyzed with ProcartaPlex 6 Plex (eBioscience) according to the manufacturer's instructions. The cytokine concentrations were corrected for the cell number. Tregs B were able to significantly reduce both IFN-ϒ and TNF-α secretion by T_{con} (p<0.05) in a 1:1 co-culture. Average of 3 replicates, student *t* test, **P* < 0.05. Error bars are standard error of mean.

B) Pairwise comparison of TCR repertoire overlaps. The color shading reflects the numerical value of the Power Geometric (PG) indices. The TCR sequences which are shared between T_{con}, Treg A and Treg B were very low with PG index less than 0.001 in all comparisons.

C&D) Gene expression profile (GEP) of Treg A and Treg B subpopulations compared to T_{con}: We have used the published GEP profile of Tregs (Ferraro et al.) as the reference list and all three T-cell populations were compared to the list which is sorted based on highly expressed genes in human Treg. Both Treg A and Treg B subpopulations were enriched with Treg related genes, in particular *IKZF2, FCRL3, FOXP3, CTLA4 and IL-2R.* However, the genes which are expressed at lower level in human Tregs were enriched in T_{con} but non of the Treg subpopulations (D) The frequency of common genes between Treg A, Treg B and references published genes (Ferraro, et al) are demonstrated in figure (E) (figure E includes genes which are highly expressed by human Tregs).

Figure 5.

A) Tregs from both AA patients and healthy donors were sensitive to IL-2 (at 0.5U/mL and 1U/mL concentration) as evident STAT5 phosphorylation after 15 and 30 minutes. Flow-cytometry result representative of 8 experiments (two HDs and six AA patients).

B) Expanded Tregs were >90% FOXP3 positive following expansion. C) There was no significant difference between AA and HD Tregs in terms of fold change increase after 4 weeks expansion (represents median fold increase of 3 HDs and 3 AA). Error bars are standard error of mean.

D) Expanded Tregs were able to suppress Tcon proliferation in both autologous and allogeneic settings (criss-cross assay) (1:1 Treg/Tcon ratio after 96 hours culture). It is noticeable that in this experiments, $Tcon_{AA}$ were proliferating slightly more than $Tcon_{HD}$ in the presence of expanded Tregs (6.43% v 3.86%), however this difference was not statistically significant when all replicates were compared.

Tcon were stained by violet proliferation dye (VPD). $Tcon_{AA}$: conventional T cells from AA patients, $Tcon_{HD}$: conventional T cells from healthy donors, Tr_{eAA}: expanded Tregs from AA patients, Tr_{eHD}: expanded Tregs from healthy donors.

Figure 6.

A) Overview of the human FOXP3 gene locus with the exon/intron structure in blue and the TSDR region in red. The lower panel shows the methylation statues of TSDR in HD and AA expanded Tregs compared to non-Tregs.

B) Expanded Tregs were polyclonal in both AA and HD. The normalized Shannon entropy of expanded Treg repertoire was used to calculate the degree of clonality which on average was 0.12.

C) As we did not succeed to isolate enough Tregs A and Treg B from AA patients for individual *in-vitro* expansion, due to low number of Tregs in these patients, the composition of *in-vitro* expanded Tregs were assesses by calculating the Euclidian distance between the mean expression for each parameter in Treg A and B was calculated in 24 Treg A, B (5 HDs and 19 AA samples) and 5 (2 AA and 3 HDs) *in-vitro* expanded Tregs. B cells were used as an irrelevant control. The following parameters which showed the highest differences between subpopulations were used for the Euclidian distance calculation: FOXP3, CD25, CD127, CD45RA, HLA-DR, CCR6, CCR4, CD69, CD27, CXCR3, CD45RO, CD4, CD20, CD95, CD161, CD28, CD152, CD7, CD279, and CD19. t-SNE1 and t-SNE2 were used for distance calculation (see also figure S10).

viSNE plot of expression centroids for all Treg cell subpopulations, B cells and expanded Tregs across all samples. Treg A and Treg B were automatically gated from 24 individual samples (19 samples from AA patients, 5 HDs) using the automated clustering algorithm FLOCK on a subset of 700,000 cells proportionally selected from all samples. B cells were gated from the same 24 samples in Cytobank. Expanded Tregs were from 3 HDs and 2 AA patients. Expression centroids were computed for each cell population and used as input for the dimensionality algorithm t-SNE

as implemented in the tool *cyt* (see Materials & Methods for more details). Each dot in the plot represents one particular cell population in a particular sample. Expression values were asinh-transformed using a cofactor of 5. Using a one tail Welch Two Sample T-test we can reject the null hypothesis that the distance between Treg A and expanded Tregs is lower than Treg B ($p<2.2 \times 10^{-16}$) which suggests that expanded Tregs are more similar to subpopulation B than A.

Figure 7.
Graphical abstract: AA patients with higher number of Treg B prior to IST are more likely to respond to therapy. Following response to IST, responder patients have higher number of Treg B compared to non-responders. Treg B are enriched with cell-cycle related proteins and more likely to enter the cell-cycle compared to Treg A subpopulations. *In-vitro* expanded Tregs are also phenotypically closer to Tregs B than Treg A.

Figures (figures are best viewed in color)

Figure 1.

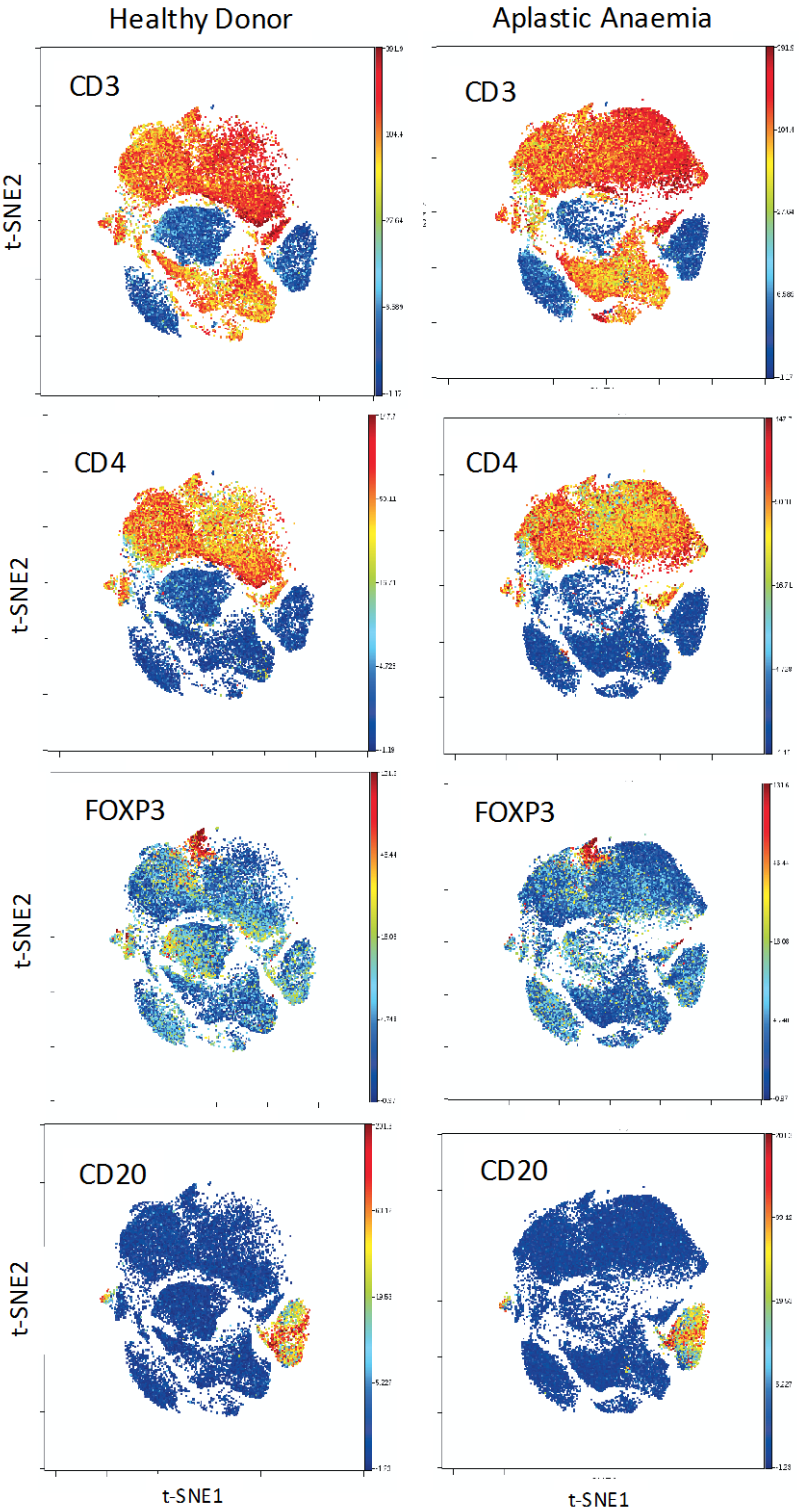

Figure 2 (A-F).

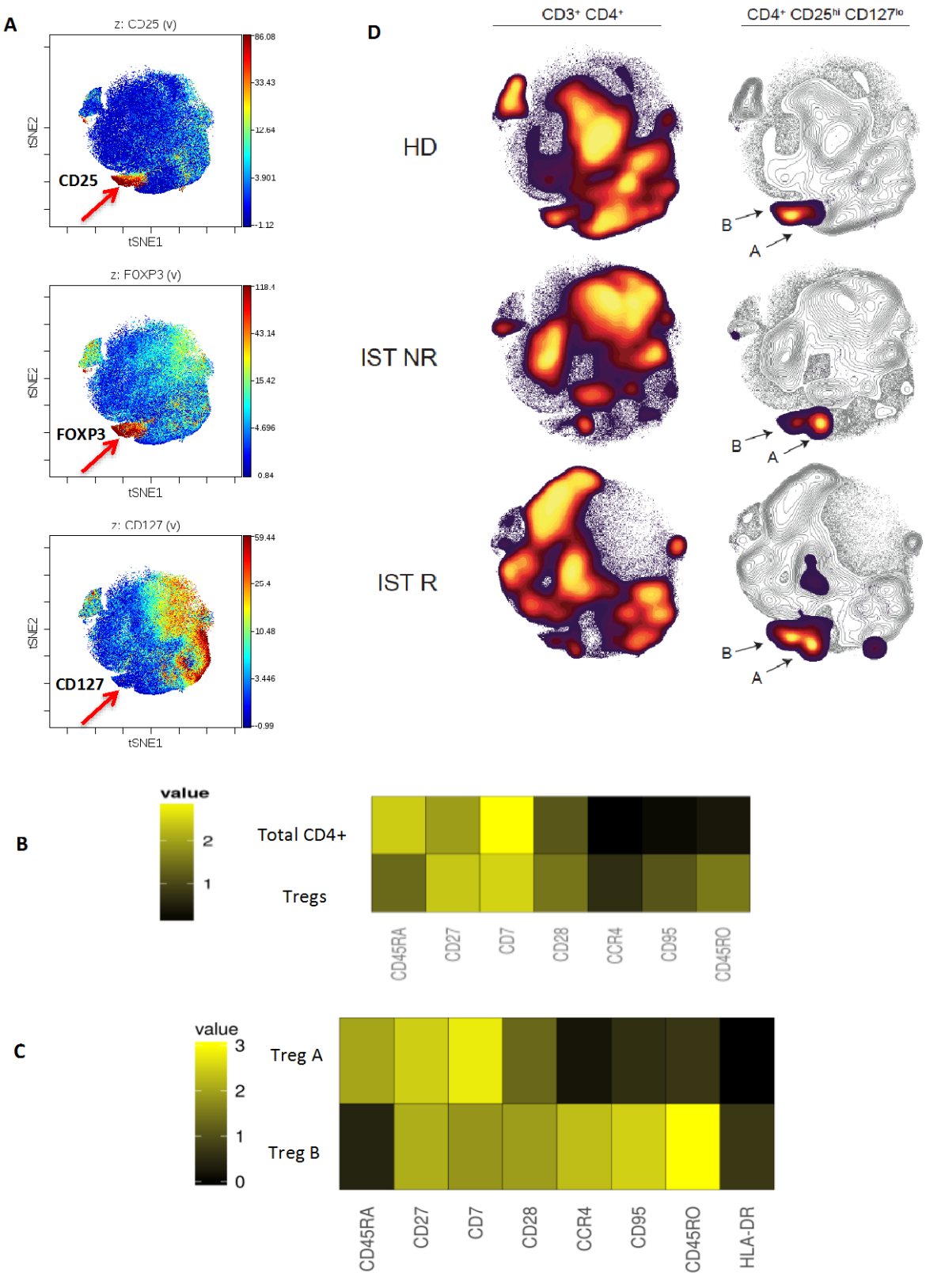
A
z: CD25 (v)
86.08
33.43
12.64
3.901
1.12
tSNE2
CD25
tSNE1
z: FOXP3 (v)
118.4
43.14
15.42
4.696
0.84
tSNE2
FOXP3
tSNE1
z: CD127 (v)
59.44
25.4
10.48
3.446
0.99
tSNE2
CD127
tSNE1
D
CD3+ CD4+
CD4+ CD25hi CD127lo
HD
IST NR
IST R
B
A
B
value
2
1
Total CD4+
Tregs
CD45RA
CD27
CD7
CD28
CCR4
CD95
CD45RO
C
value
3
2
1
0
Treg A
Treg B
CD45RA
CD27
CD7
CD28
CCR4
CD95
CD45RO
HLA-DR

E

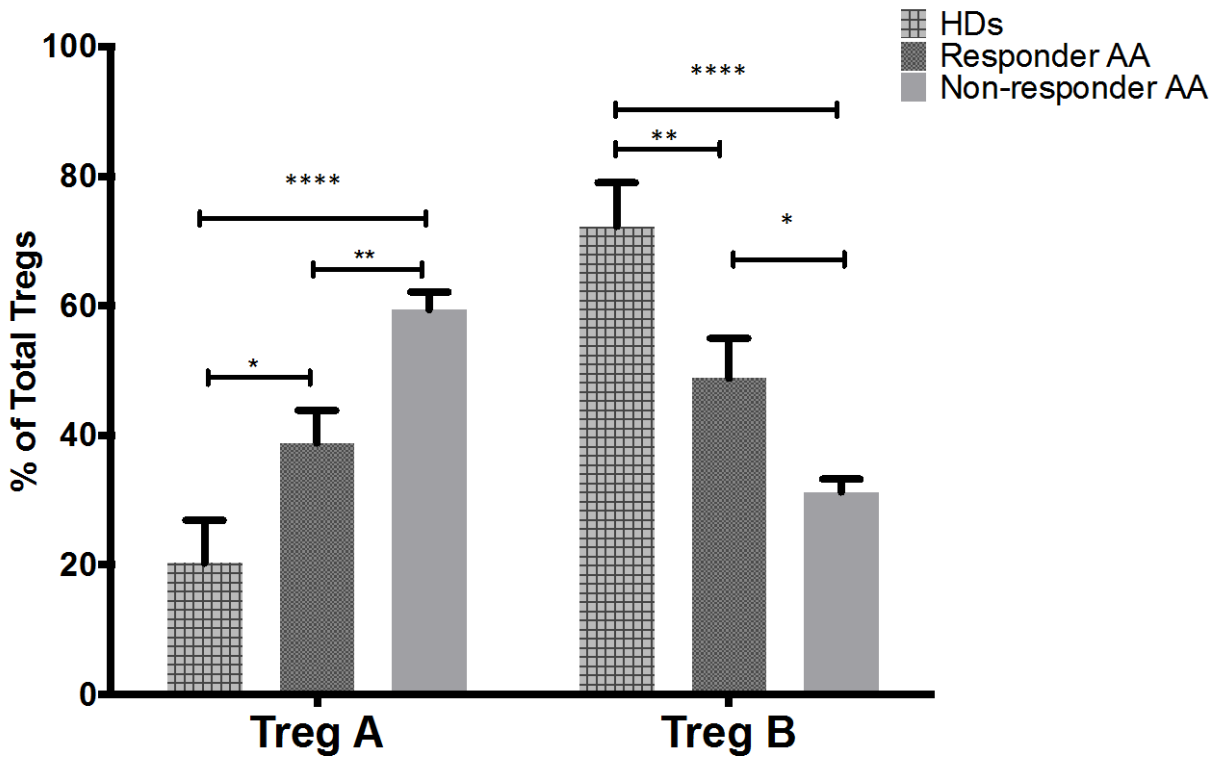
HDs
Responder AA
Non-responder AA
% of Total Tregs
100
80
60
40
20
0
****
**
*
****
**
*
Treg A
Treg B

F

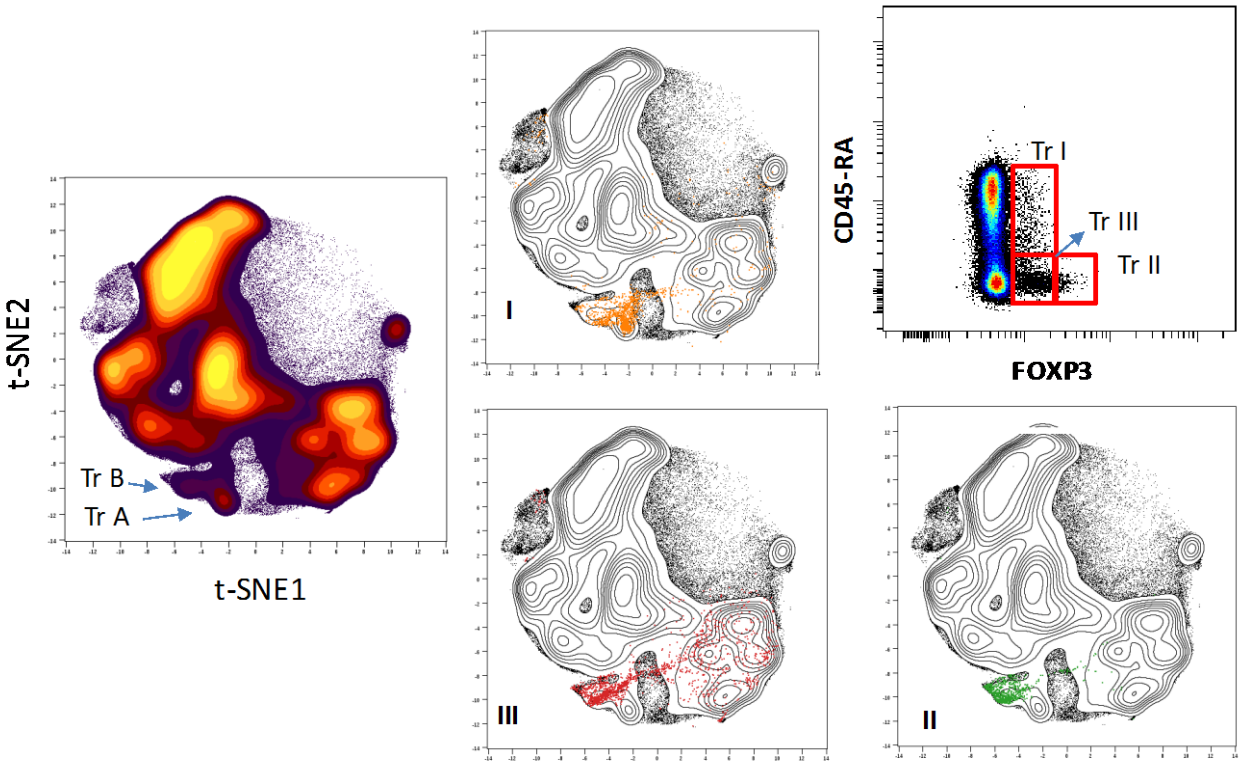
t-SNE2
t-SNE1
Tr B
Tr A
I
III
II
CD45-RA
FOXP3
Tr I
Tr III
Tr II

Figure 3 (A-E).

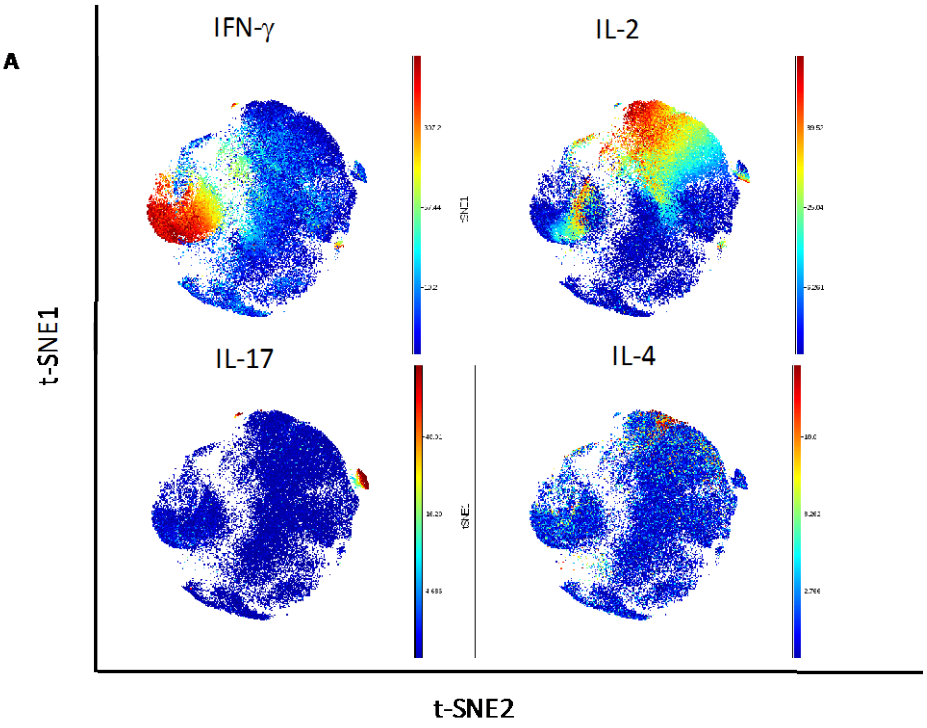
A
IFN-γ
IL-2
IL-17
IL-4
t-SNE1
t-SNE2

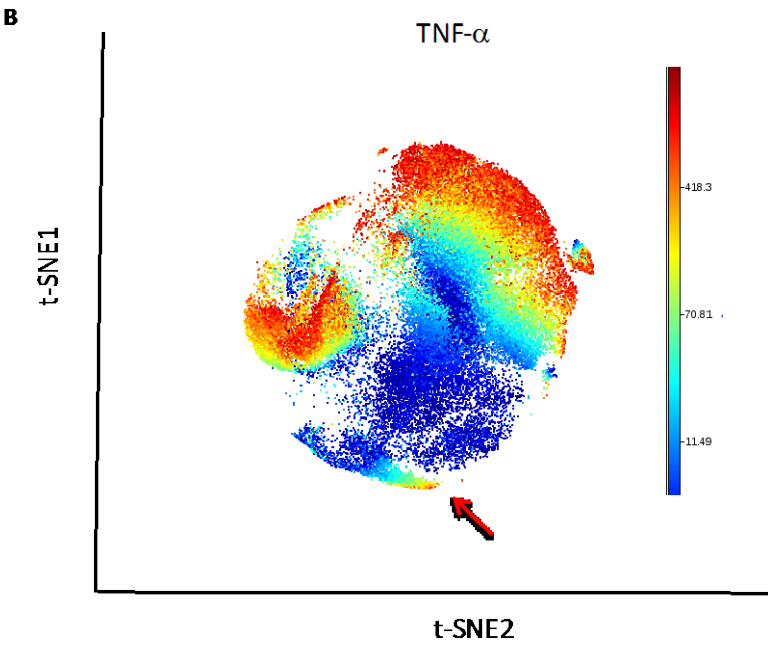
B
TNF-α
418.3
70.81
11.49
t-SNE1
t-SNE2

C

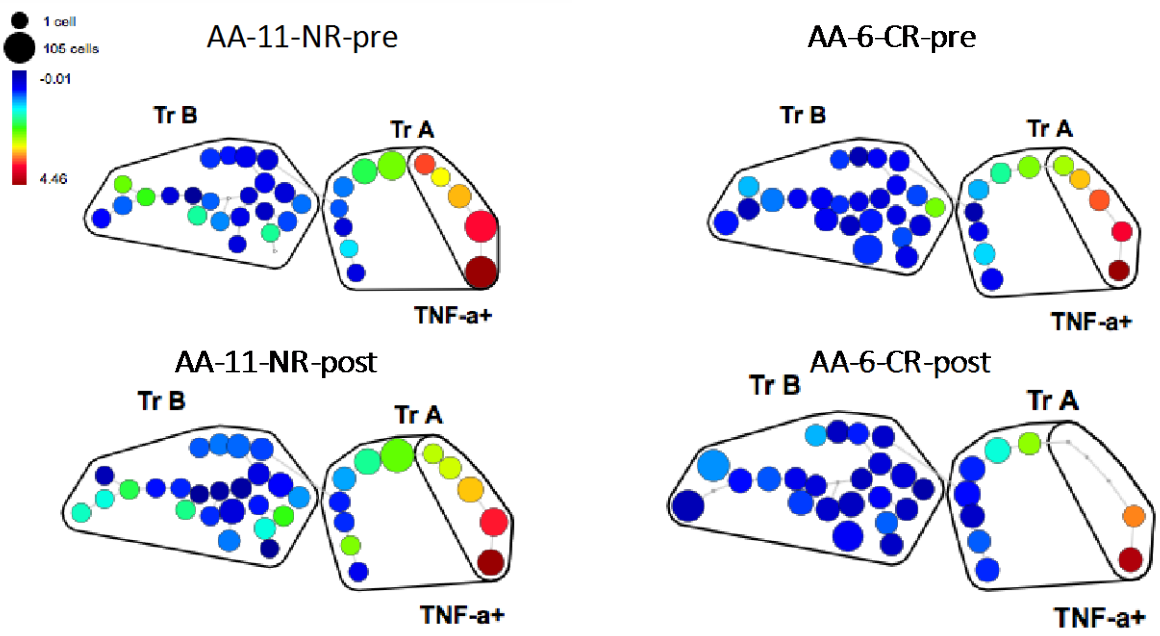
1 cell
105 cells
-0.01
4.46
AA-11-NR-pre
Tr B
Tr A
TNF-a+
AA-6-CR-pre
Tr B
Tr A
TNF-a+
AA-11-NR-post
Tr B
Tr A
TNF-a+
AA-6-CR-post
Tr B
Tr A
TNF-a+

D

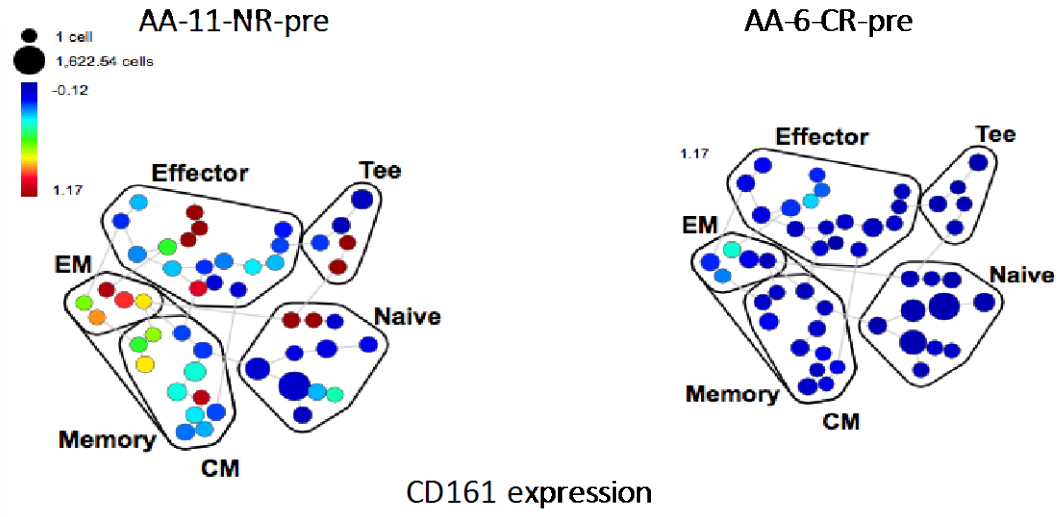
AA-11-NR-pre
1 cell
1,622.54 cells
-0.12
1.17
Effector
Tee
EM
Naive
Memory
CM
AA-6-CR-pre
1.17
Effector
Tee
EM
Naive
Memory
CM

E

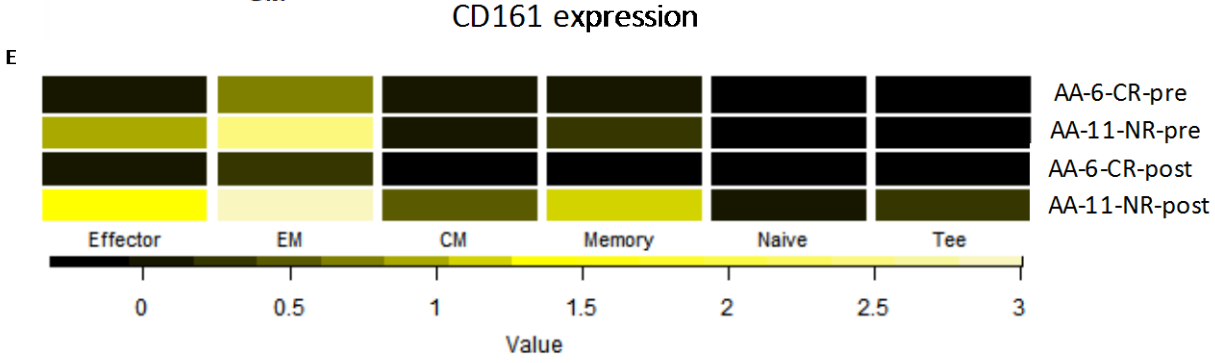
CD161 expression
AA-6-CR-pre
AA-11-NR-pre
AA-6-CR-post
AA-11-NR-post
Effector
EM
CM
Memory
Naive
Tee
0
0.5
1
1.5
2
2.5
3
Value

Figure 4 (A-E).

A

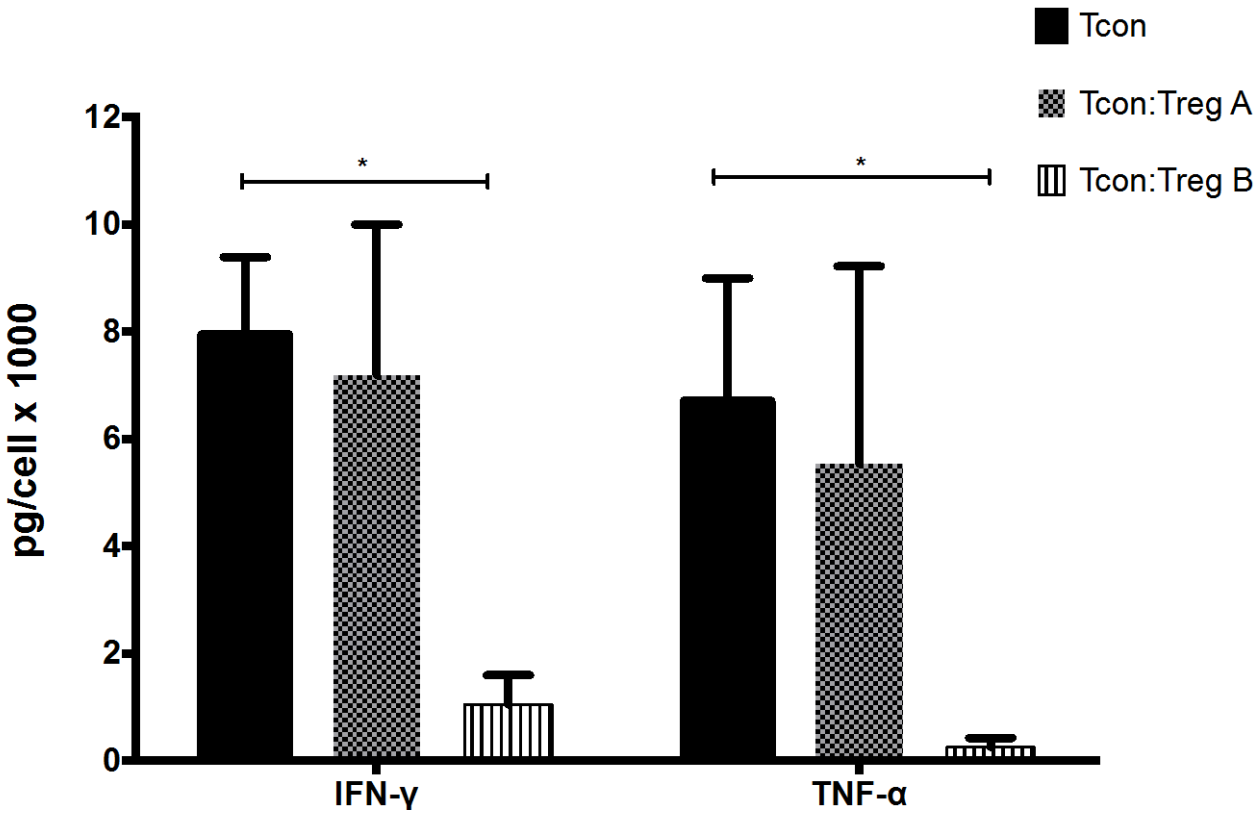
Tcon
Tcon:Treg A
Tcon:Treg B
pg/cell x 1000
12
10
8
6
4
2
0
*
*
IFN-γ
TNF-α

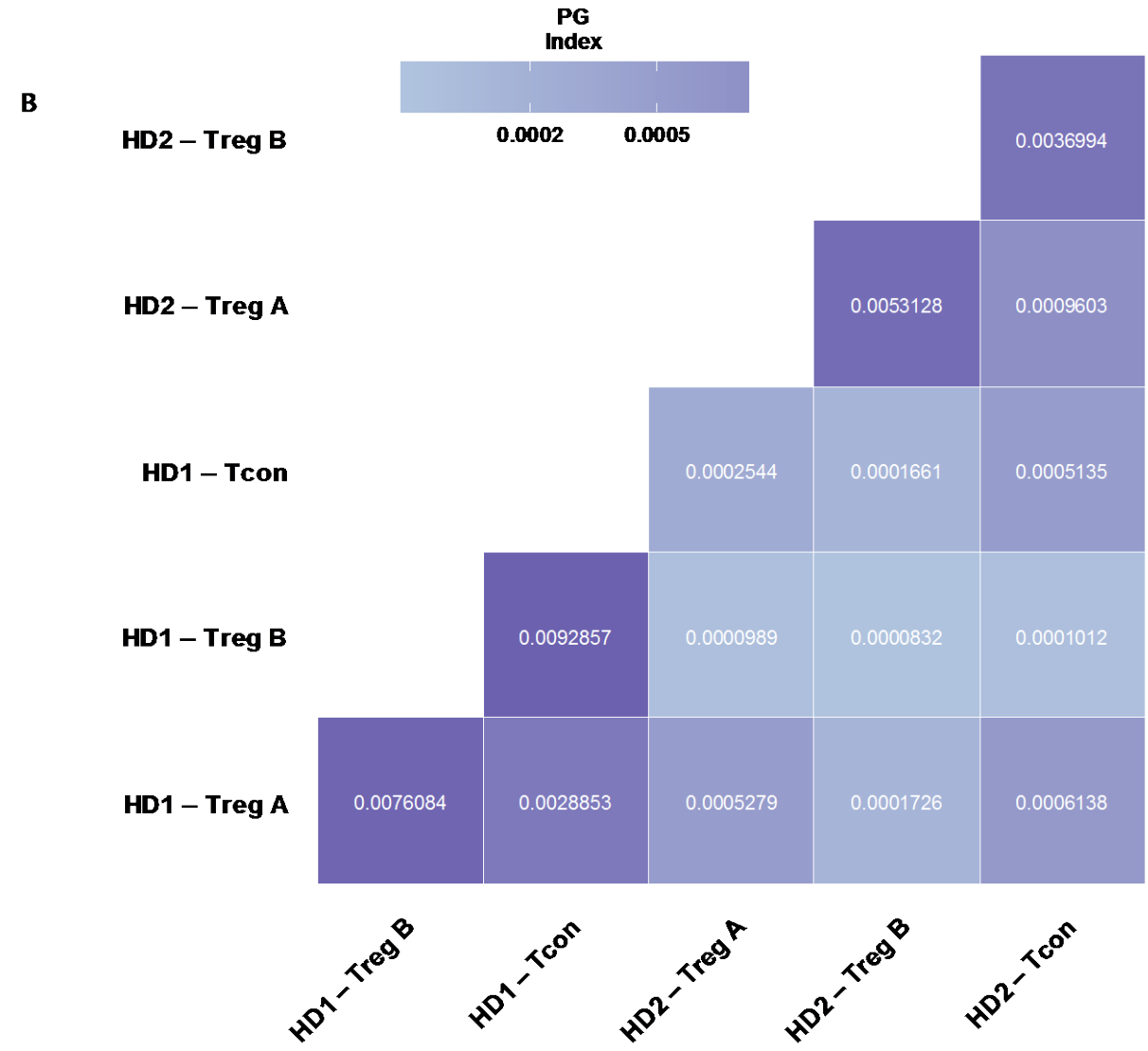
B
PG
Index
0.0002
0.0005
HD2 – Treg B
HD2 – Treg A
HD1 – Tcon
HD1 – Treg B
HD1 – Treg A
0.0036994
0.0053128
0.0009603
0.0002544
0.0001661
0.0005135
0.0092857
0.0000989
0.0000832
0.0001012
0.0076084
0.0028853
0.0005279
0.0001726
0.0006138
HD1 – Treg B
HD1 – Tcon
HD2 – Treg A
HD2 – Treg B
HD2 – Tcon

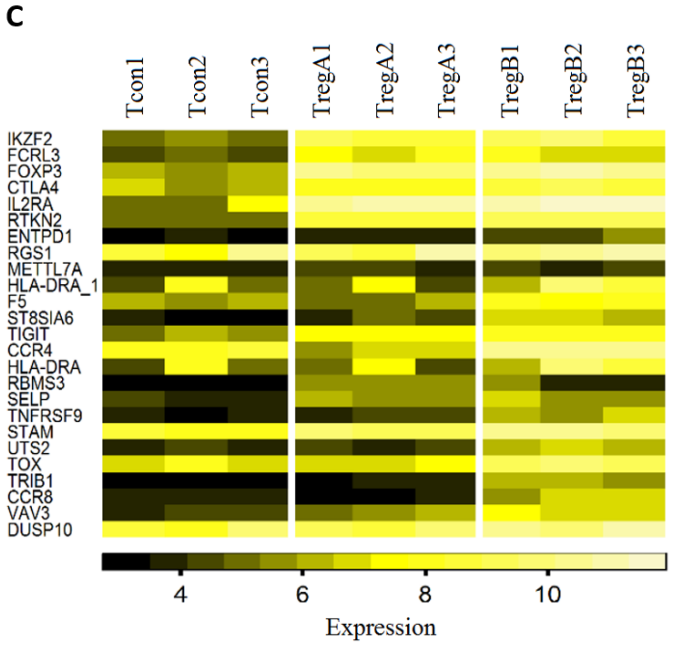
C
Tcon1
Tcon2
Tcon3
TregA1
TregA2
TregA3
TregB1
TregB2
TregB3
IKZF2
FCRL3
FOXP3
CTLA4
IL2RA
RTKN2
ENTPD1
RGS1
METTL7A
HLA-DRA_1
F5
ST8SIA6
TIGIT
CCR4
HLA-DRA
RBMS3
SELP
TNFRSF9
STAM
UTS2
TOX
TRIB1
CCR8
VAV3
DUSP10
4
6
8
10
Expression

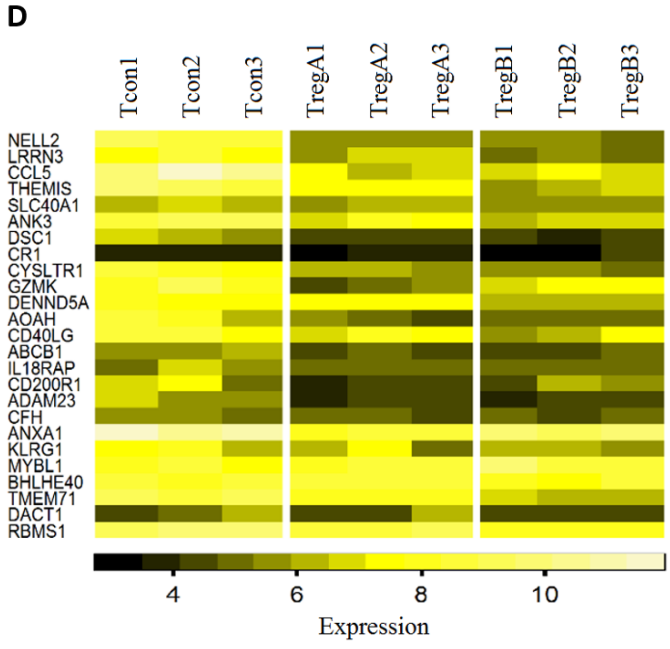
D
Tcon1
Tcon2
Tcon3
TregA1
TregA2
TregA3
TregB1
TregB2
TregB3
NELL2
LRRN3
CCL5
THEMIS
SLC40A1
ANK3
DSC1
CR1
CYSLTR1
GZMK
DENND5A
AOAH
CD40LG
ABCB1
IL18RAP
CD200R1
ADAM23
CFH
ANXA1
KLRG1
MYBL1
BHLHE40
TMEM71
DACT1
RBMS1
4
6
8
10
Expression

E

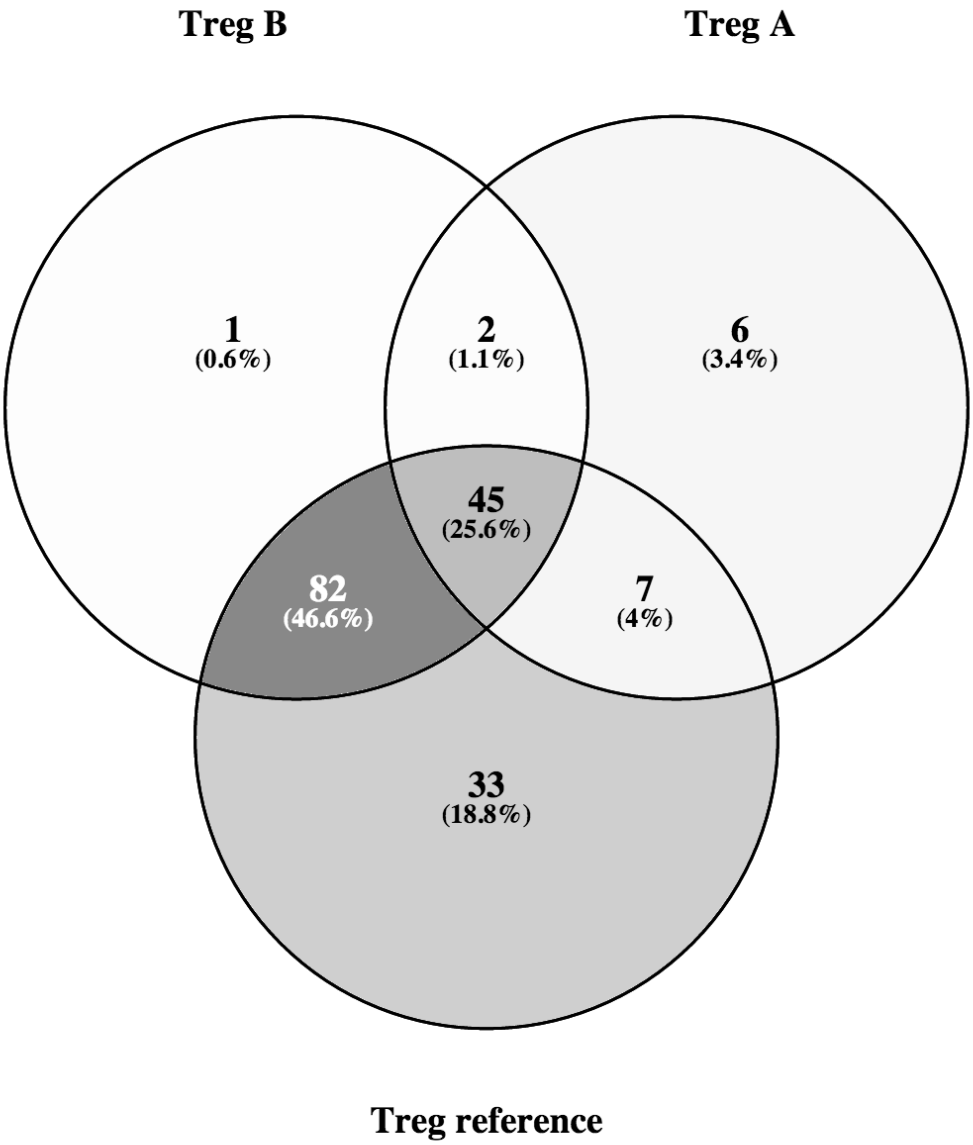

Figure 5 (A-D).

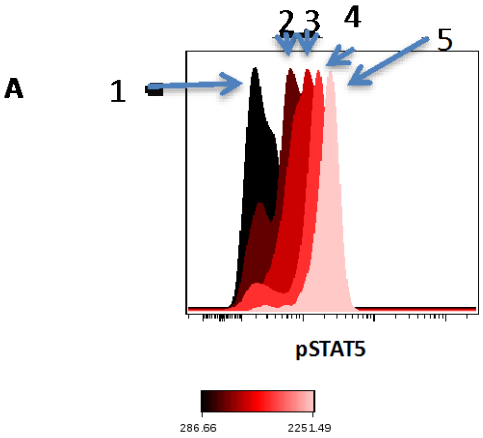

Condition	Cells	IL-2	Time
1	Tregs	0	0
2	HD Tregs	0.5 U/mL	15 min
3	AA Tregs	0.5 U/mL	15 min
4	HD Tregs	1 U/mL	30 min
5	AA Tregs	1 U/mL	30 min

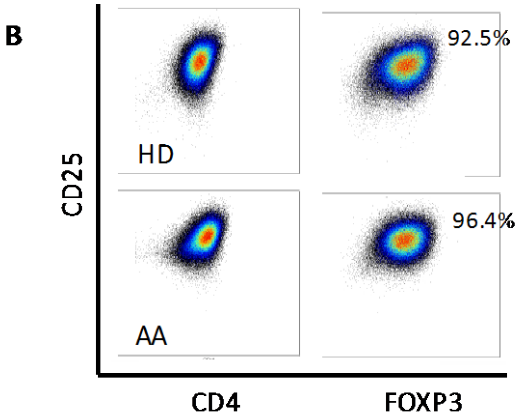

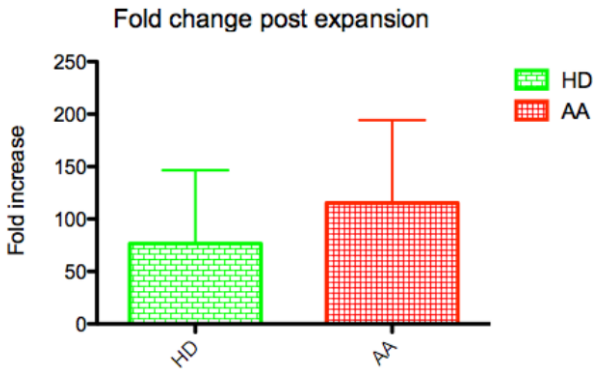

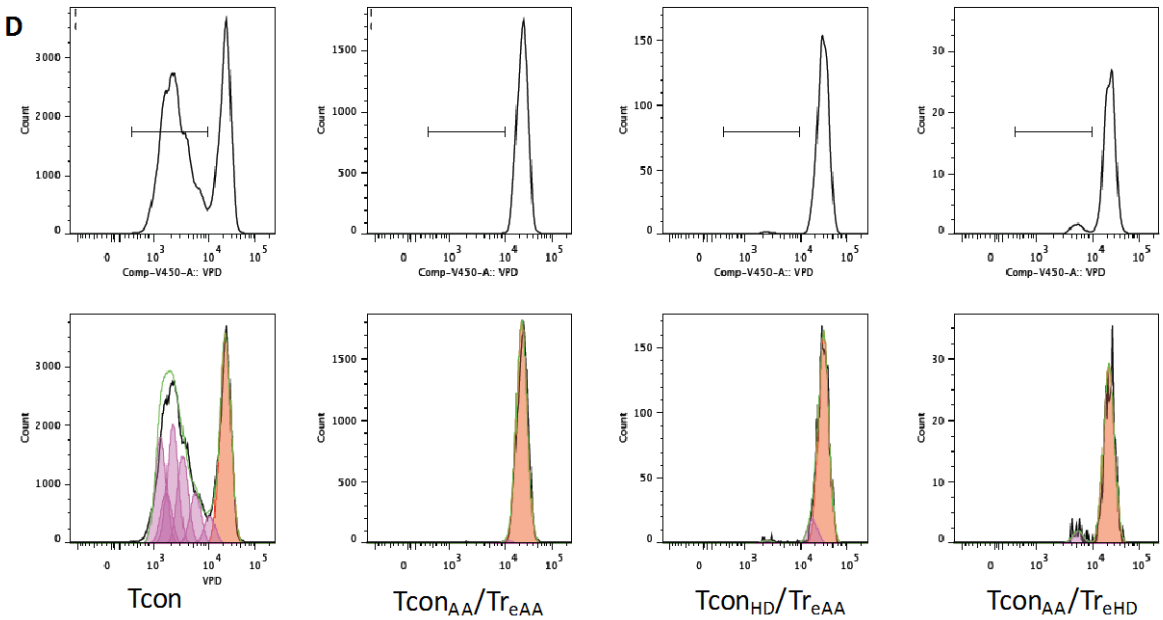

Figure 6 (A-C).

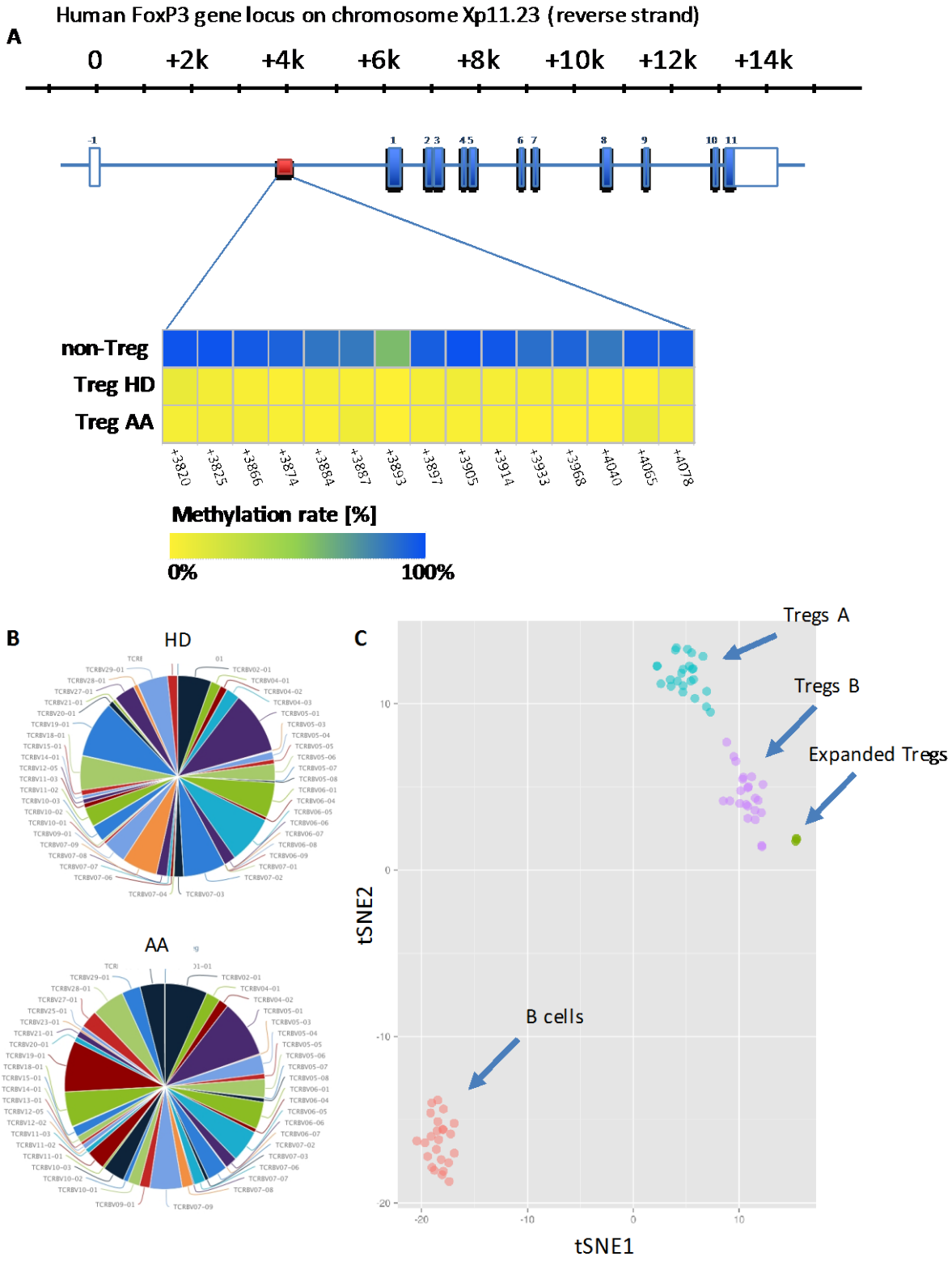
A
Human FoxP3 gene locus on chromosome Xp11.23 (reverse strand)
0
+2k
+4k
+6k
+8k
+10k
+12k
+14k
non-Treg
Treg HD
Treg AA
+3820
+3825
+3866
+3874
+3884
+3887
+3893
+3897
+3905
+3914
+3933
+3968
+4040
+4065
+4078
Methylation rate [%]
0%
100%
B
HD
AA
C
Tregs A
Tregs B
Expanded Tregs
B cells
tSNE1
tSNE2

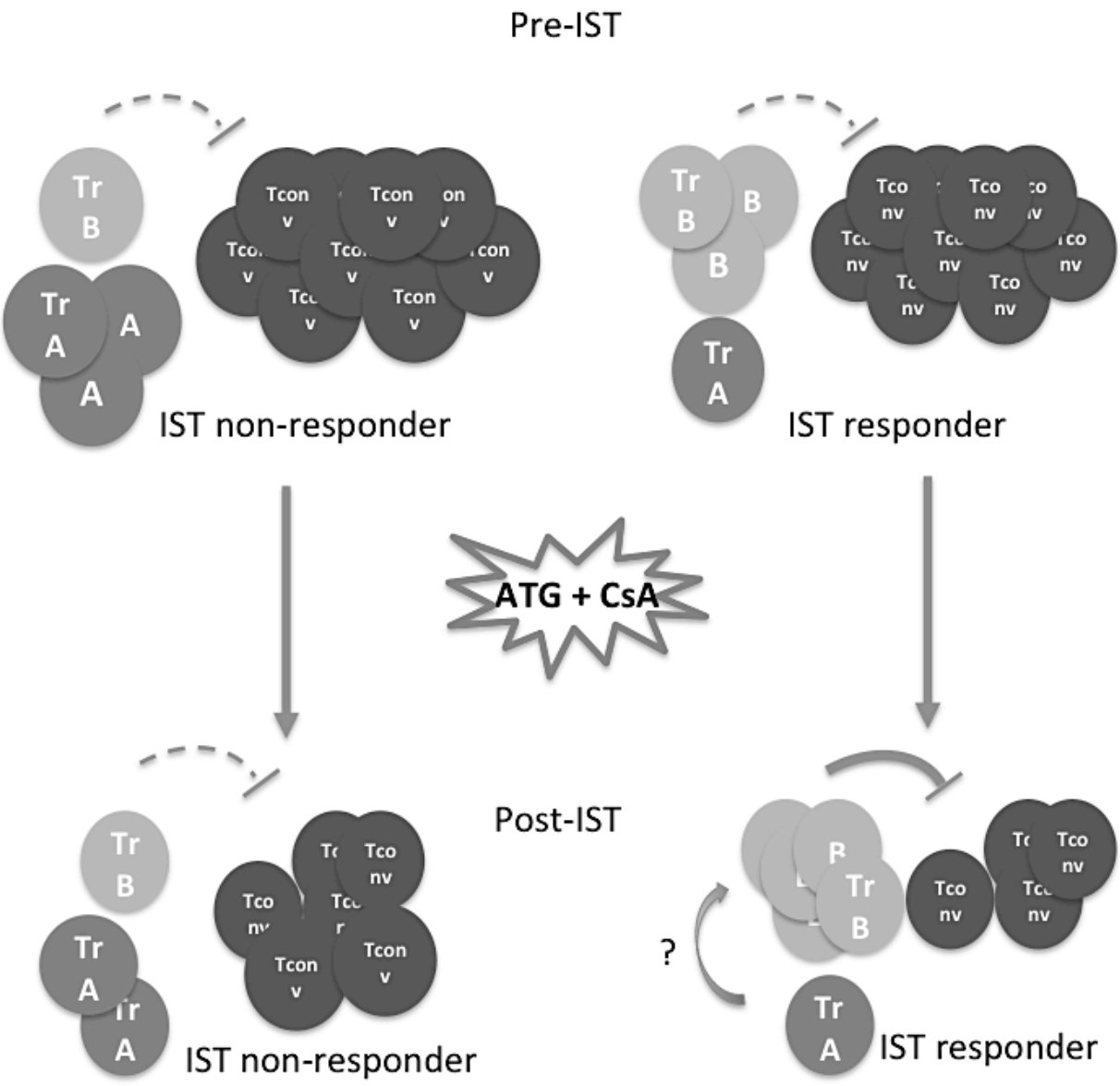

TrA: Treg A
TrB: Treg B
T_{conv}: Conventional $CD4^+$ T cells
IST: Immunosuppressive Therapy

Figure 7